

Structure–Activity Relationship Among Purpurinimides and Bacteriopurpurinimides: Trifluoromethyl Substituent Enhanced the Photosensitizing Efficacy

Amy Gryshuk,^{†,‡} Yihui Chen,[†] Lalit N. Goswami,[†] Suresh Pandey,[†] Joseph R. Missert,[†] Tymish Ohulchanskyy,[§] William Potter,[†] Paras N. Prasad,[§] Allan Oseroff,[‡] and Ravindra K. Pandey^{*,†,§}

Chemistry Division, PDT Center, and Department of Dermatology, Roswell Park Cancer Institute, Buffalo, New York 14263, and Institute of Lasers, Photonics and Biophotonics, State University of New York, Buffalo, New York 14221

Received August 29, 2006

At similar lipophilicity, compared to the nonfluorinated purpurinimide **11**, the corresponding fluorinated analog **8** with a trifluoromethyl substituent at the lower half (position-13²) of the molecule showed enhanced photosensitizing efficacy. The structural parameters established in purpurinimides (λ_{\max} : 700 nm) were successfully translated to the bacteriopurpurinimide system **19** (λ_{\max} : 792 nm) and within both series, a monotonic relationship between the lipophilicity and the in vivo PDT activity was observed. For preparing water-soluble compounds, the photosensitizers **8** and **19** were converted into the corresponding aminobenzyl–diethylenetriamine pentaacetate conjugates **23** and **26**. Acid treatment of purpurinimide **23** produced the corresponding water-soluble analog **24**. Bacteriochlorin **26** under acidic or basic conditions mainly gave the decomposition products. At similar in vivo treatment conditions (C3H mice with RIF tumors and BALB-C mice with colon-26 tumors) the water-soluble purpurinimide **24** was found to be more effective than the methyl ester analog **8**. These results suggest that besides overall lipophilicity the inherent charge of the photosensitizer also influences the PDT efficacy.

Introduction

Over the past few decades, photodynamic therapy (PDT^a) has begun to gain worldwide attention either as a primary or as an adjunctive treatment for solid cancers.^{1–3} PDT differs from other forms of therapy in that the success of the treatment is ineffective unless all the components (photosensitizer, light, and oxygen status of the tumor) are utilized in combination. In the presence of the drug-activating light, the photosensitizer undergoes a photochemical reaction in which it transfers its long-lived excited-state energy to ground state molecular oxygen residing within the tumor. This interaction produces lethal cytotoxic agents, primarily singlet oxygen (¹O₂) and other reactive oxygen species (ROS), that aid in the destruction of the malignant tissue.⁴ Therefore, the success of the treatment depends upon the tumor-selectivity and photosensitizing properties of the photosensitizer used.

A hematoporphyrin derivative (purified HpD), the first-generation photosensitizer, has most commonly been the choice for PDT treatment of various forms of cancer due to its ability to be easily synthesized and formulated.⁵ However, despite the successes of the purified version of HpD, it suffers from certain limitations due to a complex mixture of monomeric, dimeric, and oligomeric porphyrins joined with ether, ester, and carbon–carbon linkages.⁶ This complex chemical mixture makes it very difficult to make any precise conclusion as to which portion of the mixture is responsible for its photosensitizing ability. In addition, the longest wavelength absorption of 630 nm limits its penetrating ability to tumor depths of no more than 5 mm.⁷

Further, its accumulation in skin induces prolonged light sensitivity for 5–10 weeks post-PDT treatment.

To enhance the treatment of cancer and to overcome the limitations associated with a purified version of HpD, efforts in our laboratory were directed toward the synthesis of chemically pure new longer-wavelength absorbing photosensitizers⁸ related to purpurinimides and bacteriopurpurinimides. These are porphyrin-based aromatic conjugated macrocycles in which the presence of an additional imide ring fused at the *meso*-position extends its long wavelength absorption to 700 and 800 nm.⁹ Such an inherent long-wavelength characteristic should provide more efficient light penetration in tumor tissues as compared to those photosensitizers that absorb light at 630 nm.¹⁰

Previously, our group reported the structure–activity relationship (SAR) and quantitative SAR (QSAR) of a series of alkyl ether analogs of pyropheophorbide-a^{11,12} and alkyl ether derivatives of *N*-alkyl purpurinimides. The in vivo results demonstrated that the overall lipophilicity of the molecules could be easily altered by varying the length of the carbon chain, which resulted in a significant difference in photosensitizing efficacy.^{13,14}

In the pharmaceutical chemistry, fluorinated compounds in general have shown a dramatic increase in biological efficacy as compared to their nonfluorinated analogs.¹⁵ It has been illustrated that fluorine, while maintaining a comparable size to that of hydrogen (the van der Waals radii of F and H are 1.35 and 1.11, respectively) is sterically indistinguishable from a host molecule, yet maintains different biological activity.¹⁶ Having fluorine in biologically active molecules brings desirable benefits, but the trick is to introduce these fluorinated functionalities at the right place. The Schlosser group at the Swiss Federal Institute of Technology, Lausanne, have screened a series of organofluorine compounds for medical applications, and in certain structures, it was observed that introducing fluorine into the lead structure enhanced the in vivo efficacy.¹⁷

Therefore, the present study was designed to compare the photophysical and photosensitizing efficacy of a series of fluorinated versus nonfluorinated purpurinimides and bacterio-

* To whom correspondence should be addressed. Ravindra K. Pandey, Ph.D., Professor of Oncology, PDT Center, Roswell Park Cancer Institute, Buffalo, New York 13263. Phone: 716-845-3203. Fax: 716-845-8920. E-mail: ravindra.pandey@roswellpark.org.

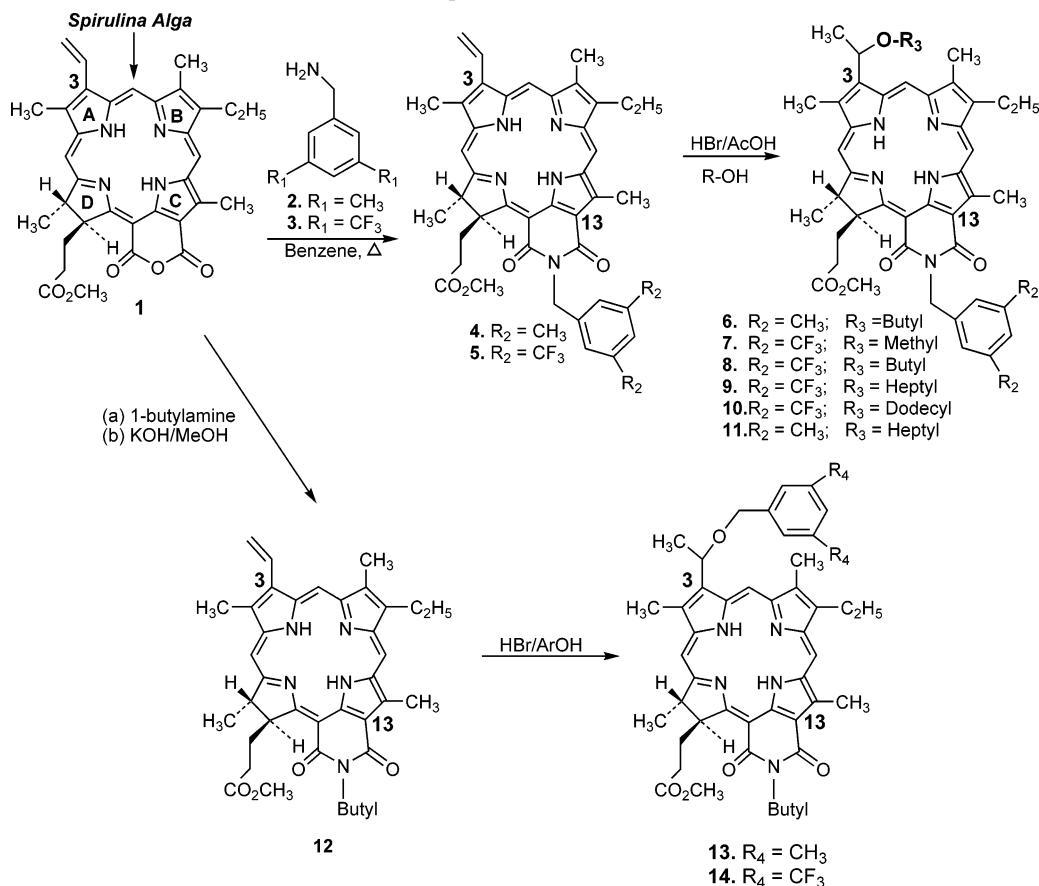
[†] Chemistry Division.

[‡] Department of Dermatology.

[§] Institute of Lasers, Photonics and Biophotonics.

^a Abbreviations: PDT, photodynamic therapy; SAR, structure–activity relationship; QSAR, quantitative structure–activity relationship; ROS, reactive oxygen species; DTPA, diethylenetriamine pentaacetate.

Scheme 1. Synthesis of Fluorinated and Nonfluorinated Purpurinimides

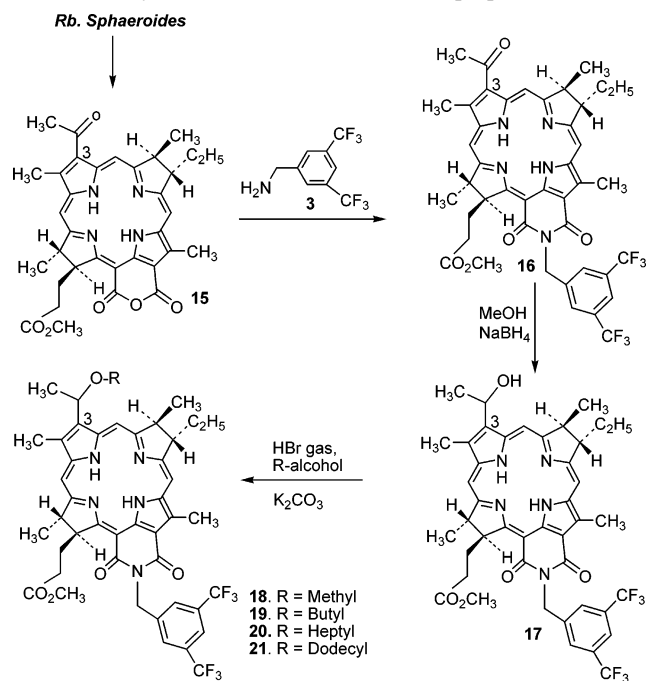


purpurinimides. Due to a close structural relationship between the purpurinimide (ring D is reduced) and the bacteriopurpurinimide systems (rings B and D are reduced), the synthetic methodology developed for purpurinimides was successfully extended for the preparation of related bacteriopurpurinimide analogs.

Results and Discussion

(i) Chemistry of Purpurinimides and Bacteriopurpurinimides: Schemes 1 and 2 display the synthetic methodology followed for the preparation of the fluorinated purpurinimides and bacteriopurpurinimides with varying lipophilicity (see Table 1 for comparative Log *P* values). The starting materials for the preparation of the desired products were extracted from *Spirulina Pacifica* (contains chlorophyll-a) and *Rb. sphaeroides* (contains bacteriochlorophyll-a). For the synthesis of purpurinimides, the methylpheophorbide-a derived from chlorophyll-a was converted into purpurin-18 methyl ester by following the literature procedure 1.¹⁸ It was then reacted with commercially available 3,5-bis(trifluoromethyl) benzyl amine 3 and refluxed in benzene. The reaction was monitored by UV-vis spectroscopy, and the resulting product exhibited a red shift from 700 nm to ~706 nm. Purpurinimide 5 was then reacted with HBr/acetic acid, and the resulting bromo-derivative was not isolated, but instead, the crude product was dried under vacuum and immediately reacted with various alkyl alcohols, differing the number of carbon units (methyl-, butyl-, heptyl-, or dodecyl-alcohol) in the presence of anhydrous potassium carbonate and dichloromethane to yield photosensitizers 7–10 of varying lipophilicity. Purpurinimides 7–10 were purified on a silica prep plate before subjecting them for *in vitro/in vivo* studies. To investigate the effect of the fluorinated versus the nonfluorinated

Scheme 2. Synthesis of Fluorinated Bacteriopurpurinimides



analog, purpurinimides 6 and 11 were also prepared by following a similar approach, except the corresponding non-fluorinated amine 2 was used as one of the starting materials instead of the fluorinated amine.

This methodology was also extended for the preparation of the fluorinated bacteriopurpurinimides, as shown in Scheme 2, in which the starting material was extracted from *Rb. sphaeroides* and converted into bacteriopurpurin methyl ester, 15. A

Table 1. Log *P* Values for the Fluorinated Purpurinimides (**7–10, 24**) and Bacteriopurpurinimides (**18–21**)

compd	7	8	9	10	18	19	20	21	24
calcd	9.43	10.91	12.13	14.67	8.82	10.30	11.83	14.38	−6.45
Log <i>P</i>									

significant red shift in long-wavelength absorption of bacteriopurpurin methyl ester **15** (815 nm) and the corresponding fluorinated bacteriopurpurinimide **16** (820 nm) were observed in organic and aqueous solutions. The product **17** (778 nm) obtained after treatment with NaBH₄ was purified via chromatography and converted into a series of bacteriopurpurinimides **18–21** by following the synthetic strategy shown in Scheme 2 (Note: HBr/AcOH was replaced with HBr gas to avoid any decomposition). As expected, similar to the purpurinimide series, varying the length of the alkyl chain at position-3 of bacteriopurpurinimide **17** also altered the overall lipophilicity of the molecule. A linear relationship between the length of *O*-alkyl chains and the overall lipophilicity was observed (see Table 1).

(ii) Water-Soluble Photosensitizers: Similar to most of the porphyrin-based compounds, the purpurinimides and bacteriopurpurinimides exhibited limited water solubility and were formulated in a 1% Tween 80/5% aqueous dextrose solution. In our attempt to prepare water-soluble analogs, the most effective fluorinated purpurinimide **8** and bacteriopurpurinimide **19** were converted into the corresponding monocarboxylic acid derivatives **22** and **25**, which on reacting with modified aminophenyl-DTPA, containing five *tert*-butylester functionalities, produced **23** and **26**, respectively, in good yield. Reaction of purpurinimide **23** with TFA at room temperature gave the desired carboxylic acid **24** in quantitative yield and was highly soluble in water (see Table 1 for Log *P* value). Under similar

reaction conditions, bacteriopurpurinimide **26** mainly produced a complex mixture of the decomposition products. Various attempts (both basic and acidic) to prepare water-soluble bacteriopurpurinimide **27** from **26** were unsuccessful (Scheme 3).

HPLC Analysis: The purity of the compounds was also ascertained by Waters HPLC system containing Waters 600 controller, and Delta 600 pump and 996 photodiode array detector. The purity was determined in both reverse and normal phase HPLC conditions. For the reverse phase, symmetry C18, 5 μm, and 4.6 × 150 mm column (Waters) was used under an isocratic setting of 100% MeOH for all the final compounds (**6–11, 13, 14, 18–21, and 26**). For the normal phase, Phenomenex Luna, 5 μm silica, and 4.6 × 250 mm column was used under a gradient setting of 100% CH₂Cl₂ for 1 min and then graded to 30% MeOH/CH₂Cl₂ over the next 30 min. Purity of compound **24** was determined in reverse phase column under isocratic 95% MeOH and 5% buffer (K₂HPO₄/KH₂PO₄ 1:1; pH = 7.0).

The photosensitizers were dissolved either in MeOH or in CH₂Cl₂ for reverse and normal phase chromatography, respectively. Solvent flow rate was kept constant at 1.00 mL/min and detector was set at 415, 545, and 700 nm for purpurinimides (**6–11, 13, 14, and 24**) and 367, 540, and 782 nm for bacteriopurpurinimides (**18–21 and 26**). The final products were obtained as a mixture of *R*- and *S*-isomers. As can be seen from Table 2, most of the compounds showed a single peak, however, in some cases, a nice separation of both the isomers was observed. The final products were found to be >95% pure (for the HPLC chromatograms of these compounds, see the Supporting Information).

Photophysical Characteristics of Purpurinimides and Bacteriopurpurinimides: The electronic absorption spectra of fluorinated purpurinimides and bacteriopurpurinimides were

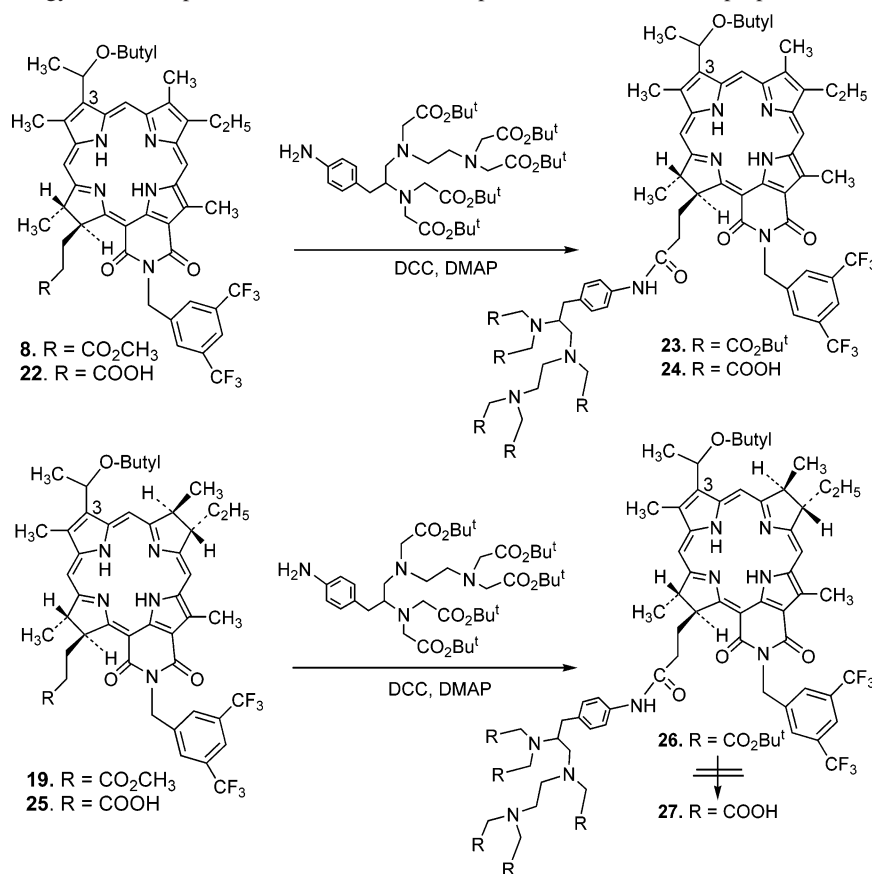
Scheme 3. Synthetic Strategy for the Preparation of Water-Soluble Purpurinimides and Bacteriopurpurinimides

Table 2. HPLC Retention Time of Purpurinimides and Bacteriopurpurinimides

cmpd	reverse phase (symmetry)		normal phase (phenomenex)	
	retention time (min)	purity (%)	retention time (min)	purity (%)
6	24.96	96.7	14.00	96.1
7	13.48	98.9	13.93	96.2
8	21.83	98.2	14.32	98.5
9	35.93	98.1	6.90, 7.34	98.5
10	67.01, 69.98	99.4	5.61, 6.03	97.9
11	41.00	95	14.50	98.8
13	26.02	97.2	14.07	99.3
14	22.97	96.6	14.09	95.6
18	3.91	95	14.05	99.8
19	16.30, 17.60	95.9	10.05	97.4
20	26.28, 28.04	99.9	10.95	99.4
21	48.44, 55.82	95	10.43, 10.91	96.8
24	4.79	95	not suitable	
26	18.77, 20.47	96	21.61	94.7

determined in anhydrous THF. The representative examples from each series are shown in Figure 1. As can be seen, the purpurinimides (i.e., **7–10**) displayed a characteristic Soret band at ~ 417 nm, with various Q-bands and a characteristic long wavelength absorption peak at ~ 701 nm ($\epsilon = 58\,000$ in THF), whereas the bacteriopurpurinimides (i.e., **18–21**) displayed a characteristic Soret band at ~ 368 and 417 nm, with various Q-bands and a characteristic long wavelength absorption peak at ~ 783 nm ($\epsilon = 40\,530$ in THF). The fluorescence spectra of purpurinimide **8** and bacteriopurpurinimide **19** are shown in Figure 2A,B, respectively, and as can be seen compared to purpurinimide, the bacteriopurpurinimide exhibited weaker absorptions. In both series, on exciting the longest wavelength absorption, this produced a small difference (Stokes shift) between the respective absorption and the emission peaks.

Steady-state measurements for the singlet oxygen ($^1\text{O}_2$) generation of **8** and **19** were performed at room temperature using the Fluorolog-3 Spectrofluorometer (Jobin Yvon). The $^1\text{O}_2$ yields were determined by normalizing the results to Rose Bengal, a known singlet oxygen producer ($Q_\Delta = 0.80$ at 1270 nm).¹⁹ The graph below (Figure 3) displayed the differences in $^1\text{O}_2$ generation between purpurinimide **8** and bacteriopurpurinimide **19**. As a representative of the purpurinimide series, **8** produced a $^1\text{O}_2$ yield $Q_\Delta \approx 0.60$, whereas the $^1\text{O}_2$ yield for **19** was two times lower ($Q_\Delta \approx 0.30$). According to these data, **8** with a more efficient $^1\text{O}_2$ yield may be predictive of a better PDT response.

Effect of Substituents in Photosensitizing Efficacy: (a) In Vitro Photosensitizing Efficacy. For determining the treat-

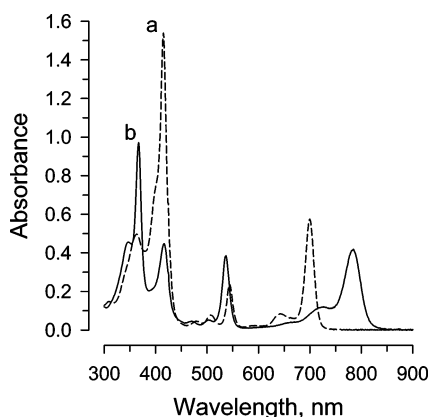


Figure 1. Electronic absorption spectra of the fluorinated photosensitizers in anhydrous THF at equimolar concentrations ($0.5\ \mu\text{M}$). (a) Purpurinimide **8** (dotted line) and (b) bacteriopurpurinimide **19** (solid line).

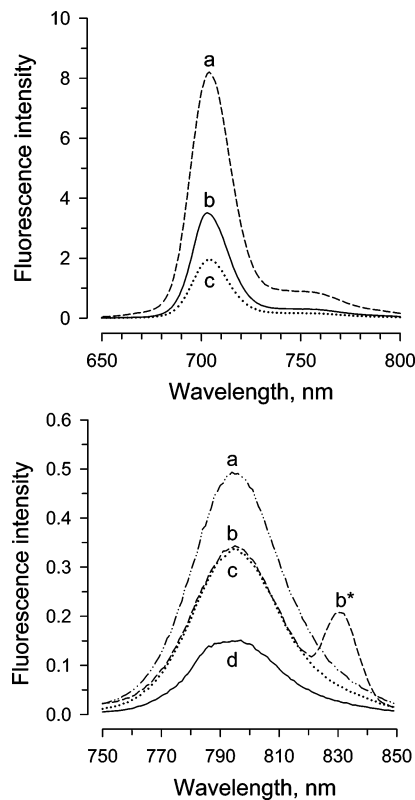


Figure 2. (A) Fluorescence spectra [only the longest wavelength emissions are shown] (a), (b), and (c) of purpurinimide **8** excited at λ_{max} : 415, 700, and 544 nm, respectively, in THF (conc. $0.5\ \mu\text{M}$). (B) Fluorescence spectra [only the longest wavelength emissions are shown] (a), (b), (c), and (d) of bacteriopurpurinimide **19** excited at λ_{max} : 366, 416, 535, and 784 nm, respectively, in THF (concd $0.5\ \mu\text{M}$). * Observed on excitation at 416 nm.

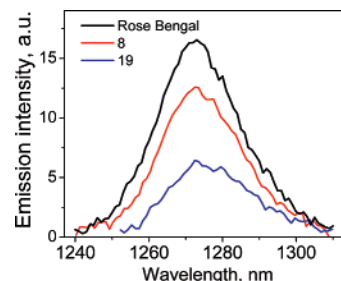


Figure 3. Singlet oxygen production efficiency of **8** and **19** referenced to Rose Bengal in methanol. Samples absorbance was matched at the wavelength of excitation ($514\ \text{nm}$). Spectra were corrected with background subtraction.

ment parameters, purpurinimide **8** was initially tested in radiation-induced fibrosarcoma (RIF) cells at three different concentrations (0.5 , 1.0 , and $2.5\ \mu\text{M}$) as a means to determine the optimum drug dose. A drug and light dose-dependent response was observed as determined by the MTT assay.²⁰ A drug concentration of $2.5\ \mu\text{M}$, together with a light dose of $4.0\ \text{J}/\text{cm}^2$, produced the best efficacy with no significant dark toxicity.

Among purpurinimides, the fluorinated photosensitizer **8** showed improved activity compared to the corresponding nonfluorinated **6**. Due to a significant difference in overall lipophilicity (**6**, 9.47; **8**, 10.91; Log P values), it was difficult to draw any conclusions. Therefore, nonfluorinated purpurinimide **11**, containing an *O*-heptyl side chain at position-3 with a Log P value of 10.99 was prepared and evaluated for PDT efficacy. As can be seen from Figure 4, **8** and **11**, with similar lipophilicity (**8**, 10.91; **11**, 10.99) showed a significant difference

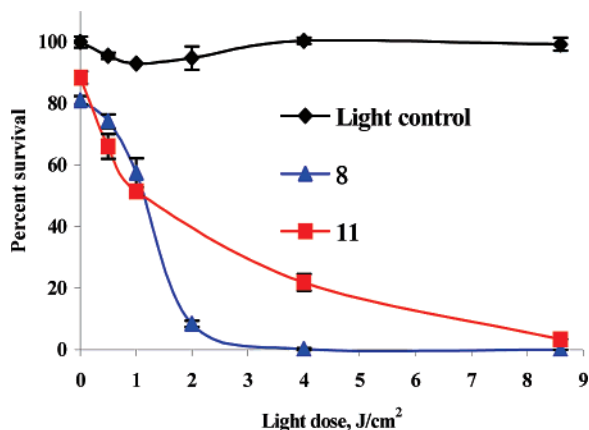


Figure 4. In vitro PDT photosensitivity of fluorinated purpurinimide **8** ($2.5 \mu\text{M}$) versus its related nonfluorinated analog **11** ($2.5 \mu\text{M}$) at similar Log P values (10.91 and 10.99, respectively). The cells were exposed to laser light at a dose of $3.2 \text{ mW}/\text{cm}^2$. Dark control: cells were incubated with photosensitizers, but not exposed to light. Light control: cells were not incubated with photosensitizers, but were exposed to laser light.

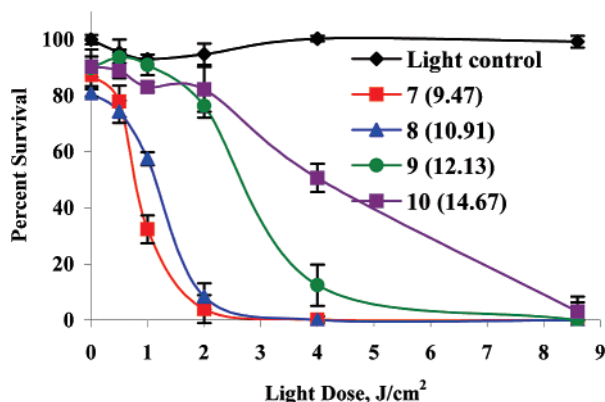


Figure 5. In vitro PDT photosensitivity of fluorinated purpurinimides **7–10** ($2.5 \mu\text{M}$) in RIF cells. The cells were exposed to laser light at a dose of $3.2 \text{ mW}/\text{cm}^2$. Dark control: cells were incubated with photosensitizers, but not exposed to light. Light control: cells were not incubated with photosensitizers, but were exposed to laser light.

in PDT photosensitivity. The fluorinated analog **8** was found to be more photosensitive than the nonfluorinated **11**.

Once the advantage of fluorinated over the nonfluorinated photosensitizers was established, our next objective was to investigate the effect of overall lipophilicity on PDT photosensitivity. Fluorinated purpurinimides **7–10** and bacteriopurpurinimides **18–21** with variable lipophilicity were evaluated in RIF under similar experimental conditions (drug concentration of $2.5 \mu\text{M}$, together with a light dose of $4.0 \text{ J}/\text{cm}^2$ to yield a fluence rate of $3.2 \text{ mW}/\text{cm}^2$). As can be seen from the results summarized in Figures 5 and 6, all photosensitizers were effective in vitro with minimal to no dark phototoxicity. However, increasing the overall hydrophobicity of the molecule reduced its photosensitizing efficacy in vitro. A likely explanation for those results may be due to differences in cellular uptake. Experiments looking at intracellular uptake and localization are currently in progress.

The in vitro results shown in Figures 5 and 6 indicate an indirect relationship between the lipophilicity and the photosensitizing efficacy. To explore things further, the biological efficacy of purpurinimide **8** (Log P 10.91) and its water-soluble analog **24** (Log P -6.45), with a drastic difference in their overall lipophilicity, were also evaluated in vitro and in vivo. The in vitro efficacy was initially determined in the murine colon

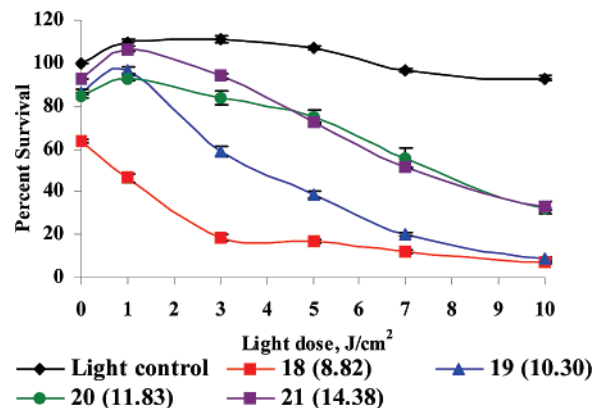


Figure 6. In vitro PDT photosensitivity of fluorinated bacteriopurpurinimides **18–21** ($2.5 \mu\text{M}$) in RIF cells. The cells were exposed to laser light at a dose of $3.2 \text{ mW}/\text{cm}^2$. Dark control: cells were incubated with photosensitizers, but not exposed to light. Light control: cells were not incubated with photosensitizers, but were exposed to laser light.

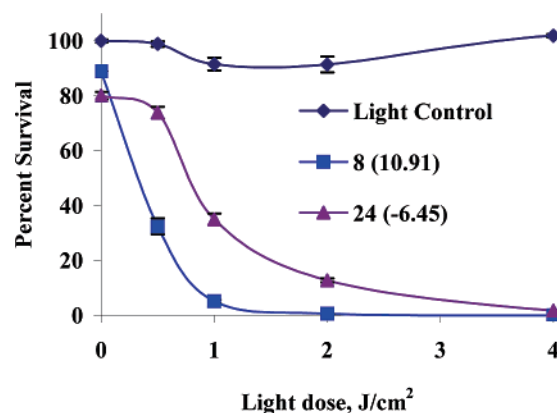


Figure 7. In vitro PDT photosensitizing efficacy of fluorinated purpurinimide **8** ($2.5 \mu\text{M}$) and its water-soluble analog **24** ($0.08 \mu\text{M}$) in colon-26 cells. The cells were exposed to laser light at a dose of $3.2 \text{ mW}/\text{cm}^2$. Dark control: cells were incubated with photosensitizers, but not exposed to light. Light control: cells were not incubated with photosensitizers, but were exposed to laser light.

carcinoma cell line (colon-26) at variable drug concentrations and a significantly lower drug concentration of water-soluble purpurinimide **24** ($0.08 \mu\text{M}$) was required to obtain a similar PDT response from purpurinimide **8** ($2.5 \mu\text{M}$) when illuminated at $4 \text{ J}/\text{cm}^2$. As shown in Figure 7, both photosensitizers produced a light-dependent PDT response with a 30-fold increase in PDT efficacy for the water-soluble analog. Such a significant increase in photosensitivity may be due to differences in intracellular uptake or localization and these studies are currently in progress. It could be hypothesized that both photosensitizers passively diffuse into the cell but that their intracellular localization differs such that **8** may be sequestered and only upon light treatment redistribute to other sensitive organelles, such as the mitochondria, which would help elicit an effective PDT-induced mechanism of cell death. On the other hand, the five carboxylic acid groups on **24**, which are anionic in nature, may allow **24** to initially localize to a more active site, such as the mitochondria.

(b) Determination of Drug-Uptake By In Vivo Reflectance Spectroscopy (IRS). The uptake of photosensitizers in tumor versus skin is an important concern in developing effective photosensitizers. The tumor and skin uptake was determined by IRS²¹ at variable time points (0–48 h postinjection) but was found to be most optimal at 24 h postinjection (Table 3). It had

Table 3. Tumor to Skin Ratios of Photosensitizers **7–10, 18–21**, and **24** at 24 h Postinjection^a

PS	In vivo (λ_{\max})	Log <i>P</i>	tumor to skin ratio	std dev (<i>n</i> = 3)
7	704	9.43	2.48	± 1.06
8	708	10.91	4.76	± 1.92
9	709	12.13	1.97	± 0.10
10	705	14.67	1.82	± 0.12
24	705	-6.45	3.68	± 0.12
18	788	8.82	1.91	± 0.33
19	791	10.30	5.30	± 2.88
20	788	11.83	6.87	± 2.40
21	791	14.38	8.89	± 3.81

^a In C3H mice bearing RIF tumors (determined by in vivo reflectance spectroscopy).

been anticipated that as the Log *P* value increased, the photosensitizer would be retained more selectively in the tumor.

(c) In Vivo Photosensitizing Efficacy. However, as can be seen from Table 3, no direct correlations were observed between the lipophilicity and photosensitizer uptake, except that the time and wavelength at which to treat in vivo had been successfully determined. Compared to the in vitro absorption characteristics in THF, the in vivo absorption of each photosensitizer exhibited a 4–5 nm red-shift (purpurinimides, ~701 nm in THF shifted to ~704–709 nm in vivo; bacteriopurpurinimides, ~783 nm in THF shifted to ~788–791 nm in vivo), which can reflect the binding of the photosensitizers to various tissue components, such as lipoproteins and human serum albumin site II.²²

(c.1) Fluorinated versus Nonfluorinated Photosensitizers as Methyl Esters: For in vivo studies, C3H mice were implanted subcutaneously with RIF tumors. A drug dose of 0.4 $\mu\text{mol/kg}$ was used to evaluate the fluorinated and nonfluorinated photosensitizers. At 24 h postinjection, the mice (10 mice/group) were treated with the specific drug-activating wavelength under the specified in vivo conditions for a total light dose of 135 J/cm^2 at a fluence rate of 75 mW/cm^2 . In the purpurinimide series, initial experiments were performed looking at the presence and position of the fluorinated substituent (Figure 8). Among the fluorinated photosensitizers (**8** and **14**; Log *P* = 10.91), **8** displayed a better PDT response. The corresponding nonfluorinated derivatives (**6** and **13**) displayed only minimal PDT response with 10% of the mice tumor-free by day 60. It was not as evident within the nonfluorinated study, but overall, it was suggested that the position of the substituent at the lower half of the macrocycle (*N*-substitution) might play a significant role in enhancing the PDT response.

Under similar treatment conditions, fluorinated purpurinimide **8** was evaluated against its nonfluorinated analog, **11**, with a similar Log *P* value (**8**, 10.91; **11**, 10.99) as a means to prove the “proof of principle” that the *N*-aryl fluorinated substituent enhanced the PDT response (Figure 9). At 60 days post-PDT, there was a significant difference ($*p < 0.0001$) in the PDT response of **8** in comparison to that of **11** (30% tumor-free for **8** versus 10% at day 60 for **11**). This experiment illustrated the

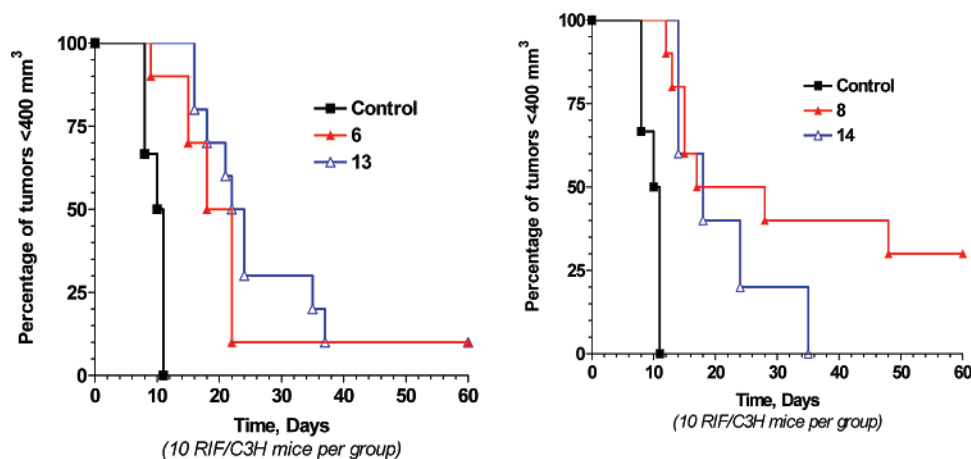


Figure 8. Kaplan–Meier plot of the in vivo photosensitizing efficacy of nonfluorinated (**6** and **13**, Log *P* = 9.43) and fluorinated (**8** and **14**, Log *P* = 10.91) photosensitizers evaluated in RIF/C3H. The mice were treated with laser light (705–708 nm, 135 J/cm^2 at 75 mW/cm^2) 24 h postinjection. The control mice were measured for tumor regrowth (<400 mm^3) and were not subjected to any photosensitizer or light.

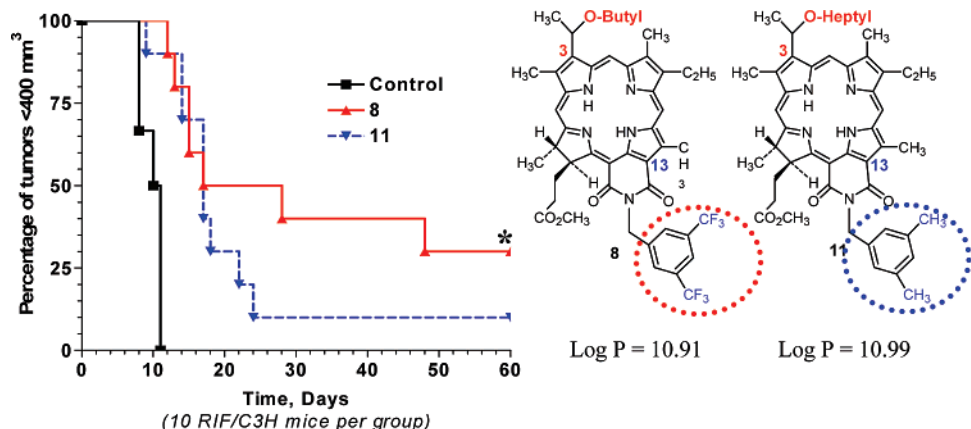


Figure 9. Kaplan–Meier plot of the in vivo photosensitizing efficacy of **8** versus its nonfluorinated analog, **11** (similar Log *P* values), evaluated in RIF/C3H. The mice were treated with laser light (705–708 nm, 135 J/cm^2 at 75 mW/cm^2) 24 h postinjection. The control mice were measured for tumor regrowth (<400 mm^3) and were not subjected to any photosensitizer or light.

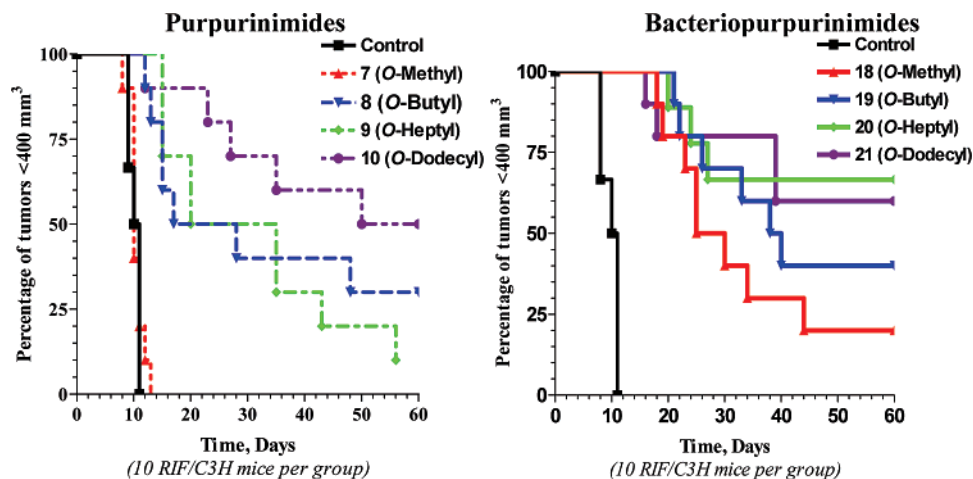


Figure 10. Kaplan–Meier plot of the in vivo photosensitizing activity of fluorinated purpurinimides (7–10) and bacteriopurpurinimides (18–21) varying in lipophilicity. The mice were treated with laser light (705–708 nm (7–10) and 788–791 nm (18–21), 135 J/cm², 75 mW/cm²) at 24 h postinjection. The control mice were measured for tumor regrowth (<400 mm³) and were not subjected to any photosensitizer or light.

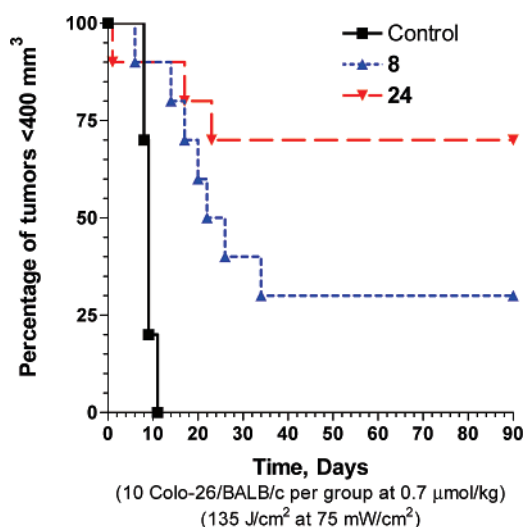


Figure 11. Kaplan–Meier plot of the in vivo photosensitizing efficacy of **8** and its corresponding water-soluble analog **24** at similar treatment conditions (24 h postinjection). The control mice were measured for tumor regrowth (<400 mm³) and were not subjected to any photosensitizer or light.

importance of the *N*-aryl functionality containing the 3,5-bis-(trifluoromethyl) benzyl groups.

Detailed biological studies with **8** and other fluorinated photosensitizers varying the length of the alkyl ether chain within both the purpurinimide (7–10) and the bacteriopurpurinimide (18–21) series were then carried out under similar PDT treatment conditions. We were interested to investigate if these new longer-wavelength fluorinated photosensitizers mimic the parabolic relationship between lipophilicity and PDT response reported within the pyrophephorbide-a series.^{11,12} Instead, a monotonic response was observed within both the fluorinated purpurinimide and the bacteriopurpurinimide series (Figure 10). As the length of the alkyl chain increased, the photosensitizing activity enhanced and the *O*-dodecyl photosensitizers (**10** and **21**) displayed the best efficacy (50 or 60% tumor-free at day 60, respectively). The effect of lipophilicity was most evident within the purpurinimide series (700 nm). Within the bacteriopurpurinimide series (800 nm), the in vivo activity of photosensitizers **20** and **21** was not significantly different ($p = 0.8020$). However, the tumor response results were comparable with what had been observed within the 700 nm series of compounds.

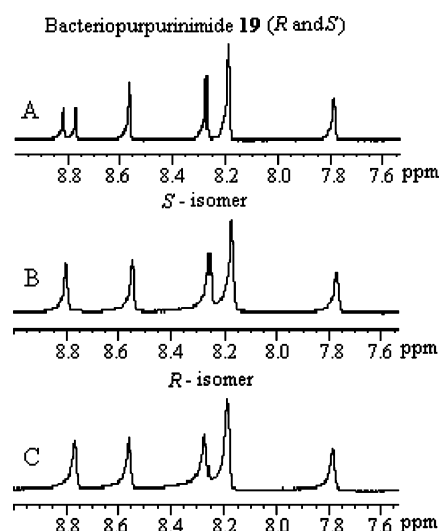


Figure 12. Partial NMR spectra of (A) Bacteriopurpurinimide **19** (mixture of *R*- and *S*-isomers), (B) isomerically pure **19S**-isomer, and (C) isomerically pure **19R**-isomer.

(c.2) Comparative Photosensitizing Efficacy of **8 and its Water-Soluble Analog **24**:** The in vivo efficacy of photosensitizers **8** and **24** was determined in both C3H mice bearing RIF tumors and BALB/c mice inoculated with colon-26 tumors at a dose of 0.7 μmol/Kg (treatment parameters: 135 J/cm², 75mW/cm² at 24 h postinjection). A similar response was observed for both model systems with the BALB/c/colon-26 data presented. According to Figure 11, both photosensitizers were effective and displayed long-term tumor cure.²³ Compared to the fluorinated purpurinimide **8**, which yielded a 30% tumor-free response at day 90, its corresponding water-soluble analog **24** displayed an enhanced tumor response with 70% of the mice tumor-free.

There may be three possible explanations for the enhanced photosensitizing efficacy of compound **24** over **8**: (i) the five carboxylic acids on **24** may be attributing to a difference in intracellular localization, (ii) the PDT-induced mechanism of action may differ between the two photosensitizers, or (iii) a difference in tumor to skin uptake may play a role. The tumor to skin ratio was evaluated in the Balb/c/colon-26 model, and surprisingly, both **24** and **8** displayed optimal uptake at 24 h postinjection. This new water-soluble fluorinated purpurinimide exhibited a greater tumor to skin ratio (5.06), which may be a

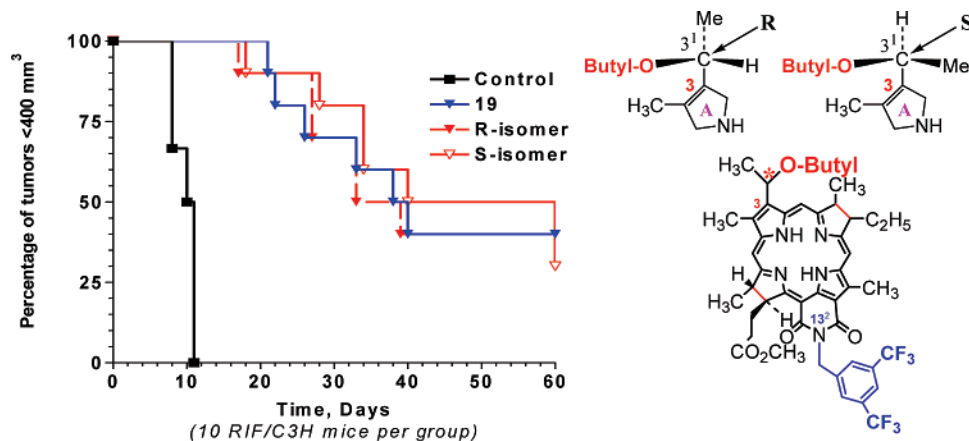


Figure 13. Kaplan–Meier plot of the in vivo photosensitizing efficacy of **19** and its corresponding **19R**- and **19S**-isomers (0.4 $\mu\text{mol/kg}$; 135 J/cm² at 75 mW/cm², 24 h postinjection). The control mice were measured for tumor regrowth (<400 mm³) and were not subjected to any photosensitizer or light.

factor for the better PDT outcome (compared to **8** with a ratio of 3.38). Detailed biodistribution studies are required to confirm this observation. These studies are currently in progress.

(c.3) Impact of Chirality on the Photosensitizing Efficacy of the Bacteriopurpurinimide System: The alkyl ether analogs of the purpurinimide and bacteriopurpurinimide systems contain a chiral center at position-3 producing a mixture of diastereomeric isomers (*R*- and *S*-configuration). For investigating the difference (if any) of the individual isomers in photosensitizing efficacy, one methyl ester photosensitizer, bacteriopurpurinimide **19**, was separated into the corresponding *R*- (**19R**) and *S*- (**19S**) isomers by HPLC. The purity of the individual isomers was confirmed by ¹H NMR (Figure 12). The absolute stereochemistry of the isomers was assigned by following the methodology reported previously.^{24,25}

Under similar treatment conditions, the PDT response of the two isomers (**19R** and **19S**) in the C3H mice bearing the RIF tumors was compared to its parent mixture **19**, and from the results summarized in Figure 13, no significant difference in photosensitizing efficacy between the two isomers (*P* values for **19R**, 0.9872, and **19S**, 0.9744) was observed.

Conclusion

The present study demonstrates the feasibility and success of altering the lipophilicity of the purpurinimide system at position-3 by varying the length of the alkyl ether chain. The structural parameters established within the purpurinimide (700 nm) series **7–10** were then translated to the bacteriopurpurinimide (800 nm) **18–21**. The in vivo photosensitizing results within both series clearly indicated the superiority of the *O*-dodecyl photosensitizers **10** and **21** in comparison to those that were less lipophilic (*O*-methyl; **7** and **18**). In contrast to the alkyl ether analogs of pyropheophorbide-a, which produced a parabolic relationship between the overall lipophilicity and the photosensitizing efficacy, a monotonic relationship was observed in both the purpurinimide and the bacteriopurpurinimide systems. Additionally, the chiral center at position-3, which produces a mixture of diastereomeric isomers, did not display significant differences (*P* = 0.9744) in PDT response when either separated (i.e., **19R** or **19S**) or left as a mixture **19**.

Most of the porphyrin-based photosensitizers, except Npe6 or LS-11, that are under various phases of clinical trials are insoluble in water, and formulating them in a suitable nontoxic solvent is a major task. In our present study, we also report the preparation of a water-soluble longer wavelength photosensitizer **24** (Log *P* = −6.45 calculated by PALLAS program). Even

with such a hydrophilic nature, the purpurinimide **24** showed a significantly higher uptake in tumor than skin (tumor to skin ratio: 5.06) at 24 h postinjection compared to that of **8** (tumor to skin ratio of 3.38). The inherent charge as well as a significant high tumor uptake could be the factors for an enhanced tumor response (70% compared to 30% produced by purpurinimide **8**). Attempts to convert bacteriopurpurinimide **26** bearing five *tert*-butylester functionalities into the corresponding penta-carboxylic acids under both acid and base conditions were unsuccessful. In a modified synthetic approach, we plan to replace the *tert*-butyl ester functionalities by the benzyl ester substituents, which on hydrogenation under controlled conditions should produce the desired water-soluble bacteriopurpurinimide. The synthesis, the site(s) of localization of the foregoing purpurinimides and bacteriopurpurinimides and the experiments to understand its correlation in mechanism(s) of cell death are currently in progress. We are also investigating the utility of these fluorinated photosensitizers as “bifunctional agents” for PDT and F-19 MR imaging.

Experimental Section

Chemistry. Purpurin-18 methyl ester **1** and bacteriopurpurin-18 methyl ester **15** were obtained from chlorophyll-a and bacteriochlorophyll-a, which in turn were extracted from *Spirulina pacifica* and *Rb. sphaeroides* by following the methodology previously reported from our laboratory.^{9,13,14} The 3,5-bis(trifluoromethyl) benzyl amine was purchased from Sigma-Aldrich and used directly. The reactions were carried out under nitrogen in degassed dried benzene and monitored by analytical thin layer chromatography (TLC). Silica gel 60 (70–230 mesh, Merck) was used for column chromatography. All the intermediates and the final compounds were characterized by UV-vis, ¹H NMR, and ¹⁹F NMR spectroscopy (chemical shifts expressed in δ ppm are relative to CDCl₃ at 7.26 ppm) and high-resolution mass spectrometry.

3,5-Dimethylbenzylamine (2). The commercially available 3,5-dimethylbenzyl bromide (0.6 g, 3 mmol) was reacted with 325 mg NaN₃, 350 mg (Bu)₄NHSO₄ (a phase transfer reagent), 6 mL saturated NaHCO₃, and 6 mL CHCl₃ under N₂ gas for ~24 h. The reaction was monitored periodically by analytical silica TLC in hexane/CH₂Cl₂ (60:40) and at completion was washed with water/NaHCO₃ and CH₂Cl₂. The organic layer was collected, dried over Na₂SO₄, and concentrated under vacuum, which yielded a clear oily residue identified as the corresponding azide analog. This oily residue was then hydrogenated under the presence of PtO₂ (70 mg) in MeOH (15 mL) overnight. The yellowish-colored residue 3,5-dimethylbenzylamine (**2**) was used directly for the synthesis of **4**.

Purpurin-18-N-3,5-bis(dimethyl)benzylimide (4). In brief, purpurin-18 methyl ester **1** (31 mg, 0.053 mmol) was reacted with **2**

in 9 mL benzene and refluxed overnight to produce the desired nonfluorinated purpurinimide, which exhibited a long wavelength absorption at 707 nm characteristic of the formation of a fused six-member imide ring system. The mixture was purified on a silica analytical plate using 2% acetone in CH_2Cl_2 (yield: 19 mg, 51.4%). UV-vis ($\epsilon = 53\,600$ at 705 nm in THF): 638.9 (1.22×10^3), 547.9 (1.62×10^4), 416.9 (1.43×10^5), 365.9 (4.14×10^4). ^1H NMR (400 MHz, 3 mg/1 mL CDCl_3 , δ ppm): 9.55 (s, 1H, 10H), 9.30 (s, 1H, 5H), 8.55 (s, 1H, 20H), 7.86 (dd, $J = 18.0$, 11.7, 1H, 3^1-CH=CH_2), 6.9 (d, 2H, ArH), 6.37 (t, 1H, ArH), 6.25 (d, $J = 18.0$, 1H, 3^1-CH=CH_2), 6.12 (d, $J = 11.7$, 1H, 3^1-CH=CH_2), 5.63 (m, 2H, NCH_2Ar), 5.38 (m, 1H, 17-H), 4.35 (q, $J = 7.3$, 1H, 18H), 3.80 (s, 3H, 12- CH_3), 3.77 (s, 6H, $\text{Ar}(\text{CH}_3)_2$), 3.58 (q, $J = 7.8$, 2H, $8^1\text{CH}_2\text{CH}_3$), 3.54 (s, 3H, $17^2\text{CO}_2\text{CH}_3$), 3.33 (s, 3H, 2- CH_3), 3.12 (s, 3H, 7- CH_3), 2.65–2.72 (m, 1H, 17^2CH_2), 2.30–2.45 (m, 2H, 17^1CH_2), 1.96–2.02 (m, 1H, 17^2CH_2), 1.75 (d, $J = 7.0$, 3H, 18- CH_3), 1.65 (t, $J = 7.0$, 3H, $8^1\text{CH}_2\text{CH}_3$), -0.05 (br s, 1H, NH), -0.15 (br s, 1H, NH).¹⁸

Purpurin-18-*N*-3,5-bis(trifluoromethyl)benzylimide (5). The purpurin-18 methyl ester **1** (1.0 g, 0.0017 mol) and commercially available **3** (1.5 g, 0.0062 mol) in 15 mL of benzene was stirred and refluxed for ~24 h in the dark. The reaction was monitored via analytical silica TLC in 2% acetone in CH_2Cl_2 . At completion, the mixture was concentrated under vacuum and purified on a silica column (2% acetone in CH_2Cl_2). The appropriate eluates were collected and evaporation of the solvent afforded **5** (yield: ~650 mg, 50%). UV-vis ($\epsilon = 58\,000$ at 708 nm in THF): 650.0 (5.82×10^3), 549.0 (2.34×10^4), 511.1 (2.33×10^3), 416.9 (1.35×10^5), 365.0 (4.60×10^4). ^1H NMR (400 MHz, 3 mg/1 mL CDCl_3 , δ ppm): 9.53 and 9.30 (each s, 1H, for 10-H and 5-H), 8.55 (s, 1H for 20-H), 8.24 (s, 2H, 2 \times ArH), 7.81 (s, 1H, 1 \times ArH), 6.21 (dd, $J = 17.44$, 12.83 Hz, 1H), 5.77 (m, 2H, $\text{N-CH}_2\text{Ar}$), 5.33 (d, $J = 7.4$ Hz, 1H, 17-H), 4.35 (m, $J = 6.12$ Hz, 1H, 18-H), 3.80 (s, 4H), 3.55 (s, 6H), 3.33 (s, 4H), 3.12 (s, 4H), 2.171 (s, 1H), 1.964 (d, 2H), 1.77 (d, $J = 8.6$ Hz, 4H), 1.64 (t, $J = 6.8$, 5H), 1.54 (s, 4H), 0.114 (br s, 1H, 2 \times NH). Mass calculated for $\text{C}_{43}\text{H}_{39}\text{N}_5\text{O}_4\text{F}_6$, 803.29; found, 804.2 (M + H).¹⁸

3-Devinyl-3-(1-butoxyethyl)-purpurin-18-*N*-3,5-bis(dimethyl)benzylimide (6). Compound **4** (19 mg, 0.027 mmol) was reacted with 1.5 mL 30% HBr in acetic acid as a means to activate the vinyl group. After 1 h of stirring, the reaction was stopped and the excess HBr/acetic acid was removed via high vacuum. To the intermediate bromo analog was added 0.5 mL of butanol, 10 mg of anhydrous K_2CO_3 , and 2 mL of dry CH_2Cl_2 . After ~1 h of stirring under N_2 gas, the reaction was stopped and washed with water and CH_2Cl_2 , and the organic layer was collected, dried over Na_2SO_4 , and filtered. The filtrate was rotovapped to dryness and aprotroped with water (if necessary) to remove any unreacted alcohol. The crude compound was purified on analytical silica plates using a hexane/ethyl acetate (70:30) solvent system, where it exhibited a peak absorbance at 699 nm in CH_2Cl_2 (yield: 12 mg, 57.7%). Log $P = 9.47$. UV-vis ($\epsilon = 53\,600$ at 698 nm in THF): 640.9 (7.68×10^3), 543.0 (2.10×10^4), 507.0 (7.97×10^3), 478.0 (4.80×10^3), 415.1 (1.44×10^5), 364.0 (4.72×10^4). ^1H NMR (400 MHz, 3 mg/1 mL CDCl_3 , δ ppm): 9.75 and 9.64 (each s, 1H, for 10H and 5H), 8.53 (s, 1H, for 20H), 7.33 (s, 2H, 2 \times ArH), 6.89 (s, 1H, ArH), 5.78 (q, $J = 6.8$ Hz, 1H, 3^1CH), 5.62 (q, $J = 12.8$, 2H, NCH_2Ar), 5.42 (d, $J = 8.2$ Hz, 1H, 17H), 4.33 (q, $J = 7.2$ Hz, 1H, 18H), 3.83 (s, 3H, 12 CH_3), 3.60–3.72 (m, 4H, 8^1CH_2 and $3^1\text{-OCH}_2\text{C}_3\text{H}_7$), 3.53 (s, 3H, $17^2\text{CO}_2\text{CH}_3$), 3.30 (s, 3H, 7 CH_3), 3.18 (s, 3H, 2 CH_3), 2.62–2.70 (m, 1H, 17^2H), 2.24–2.44 (m, 2H, 17^1H), 2.31 (s, 6H, 2 \times Ar- CH_3), 2.05 (m, 3H, 3^1CH_3), 1.98–2.04 (m, 1H, 17^2H), 1.75 (d, $J = 6.8$ Hz, 3H, 18 CH_3), 1.64–1.78 (m, 2H, $3^1\text{-OCH}_2\text{CH}_2\text{CH}_2\text{CH}_3$), 1.67 (t, $J = 7.8$ Hz, 4H, 8^2CH_3), 1.40–1.50 (m, 2H, $3^1\text{O}(\text{CH}_2)_2\text{CH}_2\text{CH}_3$), 0.862 (m, $3^1\text{O}(\text{CH}_2)_3\text{CH}_3$), -0.05 (br s, 1H, NH), -0.15 (br s, 1H, NH). Mass calculated for $\text{C}_{47}\text{H}_{55}\text{N}_5\text{O}_5$, 769.42; found, 792.4 (M + Na). HRMS calculated, 769.4209; found, 769.4256.

3-Devinyl-3-(1-methoxyethyl)-purpurin-18-*N*-3,5-bis(trifluoromethyl)benzylimide (7). Compound **5** (125 mg, 0.16 mmol) was reacted with 3 mL of 30% HBr in acetic acid for ~2 h. The excess

acetic acid was removed via high vacuum (~1 h), yielding a dark green/purple residue. To the dry residue was added 100 mg of anhydrous K_2CO_3 , 2 mL of methanol and 1.5 mL of dry CH_2Cl_2 . The reaction was stirred at RT under N_2 gas for ~1 h. At completion, the reaction mixture was washed with water and CH_2Cl_2 , and the organic layer was collected, dried over Na_2SO_4 , and filtered. The filtrate was rotovapped to dryness, yielding a dark purple crude material. The crude material was purified on silica prep plates using a hexane/ethyl acetate (80:20) solvent system (yield: 80 mg, 59.7%). Log $P = 9.43$. UV-vis ($\epsilon = 58\,000$ at 700 nm in THF): 647.0 (1.14×10^4), 544.0 (2.63×10^4), 507.0 (1.06×10^4), 479.1 (7.71×10^3), 414.9 (1.55×10^5), 363.0 (5.53×10^4). ^1H NMR (400 MHz, 3 mg/1 mL CDCl_3 , δ ppm): 9.75 and 9.63 (each s, 1H, for 10H and 5H), 8.52 (s, 1H, for 20H), 8.25 (s, 2H, 2 \times ArH), 7.81 (s, 1H, ArH), 5.77 (m, 3H, $\text{N-CH}_2\text{Ar}$ and 3^1H), 5.34 (d, $J = 7.6$ Hz, 1H, 17H), 4.35 (q, $J = 7.2$ Hz, 1H, 18H), 3.68 (s, 3H, 12 CH_3), 3.50–3.60 (m, 8H, $17^2\text{CO}_2\text{CH}_3$, 8^1CH_2 , 3^1OCH_3), 3.31 (s, 3H, 7 CH_3), 3.19 (s, 3H, 2 CH_3), 2.64–2.74 (m, 1H, 1 \times 17^2H), 2.35–2.45 (m, 2H, 17^1H), 2.06 (m, 3H, 3^1CH_3), 1.95–2.04 (m, 1H, 1 \times 17^2H), 1.76 (d, $J = 6.8$ Hz, 3H, 18 CH_3), 1.69 (t, $J = 7.4$ Hz, 3H, 8^2CH_3), 0.08 (br s, 1H, NH), 0.03 (br s, 1H, NH). ^{19}F NMR (400 MHz, 3 mg/1 mL of CDCl_3 , in reference to TFA, δ ppm): 13.28. Mass calculated for $\text{C}_{44}\text{H}_{43}\text{N}_5\text{O}_5\text{F}_6$, 835.32; found, 858.5 (M + Na). HRMS calculated (M + H), 836.3246; found, 836.3224.

3-Devinyl-3-(1-butoxyethyl)-purpurin-18-*N*-3,5-bis(trifluoromethyl)benzylimide (8). Compound **5** (200 mg, 0.25 mmol) was reacted with ~5 mL of 30% HBr in acetic acid for ~2 h. The excess acetic acid was removed via high vacuum (~45 min), yielding a dark green/purple residue. To the dry residue was added 100 mg of anhydrous K_2CO_3 , 1 mL of *n*-butanol, and 3 mL of dry CH_2Cl_2 . The reaction was stirred at RT under N_2 gas for ~1 h. At completion, the reaction mixture was washed with water and CH_2Cl_2 , and the organic layer was collected, dried over Na_2SO_4 , and filtered. The filtrate was rotovapped to dryness to yield a dark purple crude material. The crude material was purified on silica prep plates using a hexane/ethyl acetate (80:20) solvent system. The pure compound exhibited a characteristic absorption peak at 701 nm in CH_2Cl_2 (yield: 100 mg, 45.7%). Log $P = 10.91$. UV-vis ($\epsilon = 58\,000$ at 700 nm in THF): 644.1 (8.65×10^3), 544.0 (2.42×10^4), 507.9 (7.53×10^3), 478.0 (4.33×10^3), 415.1 (1.57×10^5), 364.0 (4.98×10^4). ^1H NMR (400 MHz, 3 mg/1 mL CDCl_3 , δ ppm): 9.75 and 9.63 (each s, 1H, for 10H and 5H), 8.52 (s, 1H, for 20H), 8.25 (s, 2H, 2 \times ArH), 7.81 (s, 1H, ArH), 5.77 (m, 3H, $\text{N-CH}_2\text{Ar}$ and 3^1H), 5.34 (d, $J = 7.6$ Hz, 1H, 17H), 4.35 (q, $J = 7.2$ Hz, 1H, 18H), 3.84 (s, 3H, 12 CH_3), 3.69 (m, 4H, 8^1CH_2 , $3^1\text{OCH}_2\text{-C}_3\text{H}_7$), 3.31 (s, 3H, 7 CH_3), 3.19 (s, 3H, 2 CH_3), 2.68 (m, 1H, 1 \times 17^2H), 2.37 (m, 2H, 2 \times 17^1H), 2.06 (m, 3H, 3^1CH_3), 1.96 (m, 1H, 1 \times 17^2H), 1.76 (d, $J = 6.8$ Hz, 2H, 18 CH_3), 1.69 (t, $J = 7.4$ Hz, 3H, 8^2CH_3), 1.35–1.55 (m, 4H, $\text{OCH}_2(\text{CH}_2)_2\text{CH}_3$), 0.89 (m, 3H, $\text{O}-(\text{CH}_2)_3\text{CH}_3$), 0.17 (br s, 1H, NH), 0.05 (br s, 1H, NH). ^{19}F NMR (400 MHz, 3 mg/1 mL of CDCl_3 , in reference to TFA, δ ppm): 13.05. Mass calculated for $\text{C}_{47}\text{H}_{49}\text{N}_5\text{O}_5\text{F}_6$, 877.36; found, 878.3 (M + 1). HRMS calculated (M + 1), 878.3716; found, 878.3723.

3-Devinyl-3-(1-heptoxyethyl)-purpurin-18-*N*-3,5-bis(trifluoromethyl)benzylimide (9). Compound **5** (85 mg, 0.11 mmol) was reacted with 3.5 mL of 30% HBr in acetic acid for ~2 h. The excess acetic acid was removed via high vacuum (~30 min), yielding a dark green/purple residue. To the dry residue was added 19.6 mg of dry K_2CO_3 , 0.75 mL of *n*-heptanol, and 3 mL of dry CH_2Cl_2 . The reaction was stirred at RT under N_2 gas for ~1 h. At completion, the reaction mixture was washed with water and CH_2Cl_2 , and the organic layer was collected, dried over Na_2SO_4 , and filtered. The filtrate was concentrated under vacuum to yield a dark purple crude material. The crude material was purified on silica prep plates using a hexane/ethyl acetate (80:20) solvent system. The pure compound exhibited a characteristic absorption peak at 701 nm in CH_2Cl_2 (yield: 44 mg, 43.6%). Log $P = 12.13$. UV-vis ($\epsilon = 58\,000$ at 700 nm in THF): 644.0 (9.14×10^3), 544.0 (2.53×10^4), 508.0 (8.70×10^3), 480.0 (5.45×10^3), 414.9

(1.53×10^5), 363.9 (5.20×10^4). ^1H NMR (400 MHz, 3 mg/1 mL CDCl_3 , δ ppm): 9.80 and 9.57 (each s, 1H, for 10H and 5H), 8.58 (s, 1H, for 20H), 8.29 (s, 2H, 2 \times ArH), 7.86 (s, 1H, ArH), 5.75–5.93 (m, 3H, $\text{N}-\text{CH}_2\text{Ar}$ and 3^1H), 5.40 (d, $J = 7.6$ Hz, 1H, 17H), 4.40 (q, $J = 7.2$ Hz, 1H, 18H), 3.78 (s, 3H, 12CH_3), 3.62–3.75 (m, 4H, 8^1CH_2 , $\text{OCH}_2\text{C}_6\text{H}_{13}$), 3.60 (s, 3H, $17^2\text{CO}_2\text{CH}_3$), 3.36 (s, 3H, 7CH_3), 3.23 (s, 3H, 2CH_3), 2.66–2.80 (m, 1H, 1 \times 17^2H), 2.35–2.52 (m, 2H, 2 \times 17^1H), 2.10 (m, 3H, 3^1CH_3), 1.96–2.07 (m, 1H, 1 \times 17^2H), 1.84 (d, $J = 6.8$ Hz, 3H, 18CH_3), 1.75–1.81 (m, 2H, $\text{OCH}_2\text{CH}_2(\text{CH}_2)_4\text{CH}_3$), 1.69 (t, $J = 7.4$ Hz, 3H, 8^2CH_3), 1.35–1.55 (m, 2H, $\text{O}(\text{CH}_2)_2\text{CH}_2(\text{CH}_2)_3\text{CH}_3$), 1.15–1.34 (m, 6H, $\text{O}(\text{CH}_2)_3(\text{CH}_2)_3\text{CH}_3$), 0.83 (m, 3H, $\text{O}-(\text{CH}_2)_6\text{CH}_3$), 0.18 (br s, 1H, NH), 0.09 (br s, 1H, NH). ^{19}F NMR (400 MHz, 3 mg/1 mL of CDCl_3 , in reference to TFA, δ ppm): 13.03. Mass calculated for $\text{C}_{50}\text{H}_{55}\text{N}_5\text{O}_5\text{F}_6$, 919.41; found, 942.4 (M + Na). HRMS calculated (M + 1), 920.4185; found, 920.4167 (M + 1).

3-Devinyl-3-(1-dodecyoxyethyl)-purpurin-18-N-3,5-bis(trifluoromethyl)benzylimide (10). Compound **5** (204 mg, 0.25 mmol) was reacted with 3 mL of 30% HBr in acetic acid for ~ 2 h. The excess acetic acid was removed via high vacuum (~ 30 min), yielding a dark green/purple residue. To the dry residue was added 100 mg of dry K_2CO_3 , 1–1.5 mL of *n*-dodecanol, and 3 mL of dry CH_2Cl_2 . The reaction was stirred at RT under N_2 gas for ~ 1 h. At completion, the reaction mixture was washed with water and CH_2Cl_2 , and the organic layer was collected, dried over Na_2SO_4 , and filtered. The filtrate was concentrated under vacuum to yield a dark purple crude material. The excess dodecanol was aprotroped with water. Initially, the compound was purified on a silica column and then on an alumina column with CH_2Cl_2 as the solvent system to help remove the remaining alcohol. The filtrate was collected, rotavaporated to dryness, and additionally purified on silica prep plates using a hexane/ethyl acetate (80:20) solvent system. Due to the excessive purification demands, the percent yield of this compound was lower compared to the other fluorinated purpurinimides (yield: 25.8 mg, 10.4%). Log *P* = 14.67. UV-vis ($\epsilon = 58\,000$ at 700 nm in THF): 643.0 (9.45×10^3), 544.0 (2.53×10^4), 508.0 (8.66×10^3), 478.0 (5.77×10^3), 416.0 (1.60×10^5), 363.9 (5.42×10^4). ^1H NMR (400 MHz, 3 mg/1 mL of CDCl_3 , δ ppm): 9.81 and 9.53 (each s, 1H, for 10H and 5H), 8.6 (s, 1H, for 20H), 8.30 (s, 2H, 2 \times ArH), 7.87 (s, 1H, ArH), 5.77 (m, 3H, $\text{N}-\text{CH}_2\text{Ar}$ and 3^1H), 5.41 (d, $J = 6.9$ Hz, 1H, 17H), 4.42 (m, 1H, 18H), 3.75 (s, 3H, 12CH_3), 3.63–3.69 (m, 4H, $\text{OCH}_2\text{C}_{11}\text{C}_{23}$, 8^1CH_2), 3.61 (s, 3H, $17^2\text{CO}_2\text{CH}_3$), 3.36 (s, 3H, 7CH_3), 3.22 (s, 3H, 2CH_3), 2.65–2.83 (m, 1H, 1 \times 17^2H), 2.35–2.53 (m, 2H, 2 \times 17^1H), 2.12 (m, 3H, 3^1CH_3), 1.96–2.07 (m, 1H, 1 \times 17^2H), 1.85 (m, 3H, 18CH_3), 1.74–1.82 (m, 2H, $\text{OCH}_2\text{CH}_2(\text{CH}_2)_6\text{CH}_3$), 1.12–1.54 (m, 18H, $\text{OCH}_2\text{CH}_2(\text{CH}_2)_9\text{CH}_3$), 0.89 (m, 3H, $\text{O}-(\text{CH}_2)_{11}\text{CH}_3$), 0.16 (br s, 1H, NH), 0.09 (br s, 1H, NH). ^{19}F NMR (400 MHz, 3 mg/1 mL of CDCl_3 , in reference to TFA, δ ppm): 13.17. Mass calculated for $\text{C}_{55}\text{H}_{66}\text{N}_5\text{O}_5\text{F}_6$, 989.49; found, 1012.6 (M + Na). HRMS calculated (M + 1), 990.4968; found, 990.4994 (M + 1).

3-Devinyl-3-(1-heptoxyethyl)-purpurin-18-N-3,5-dimethylbenzylimide (11). By following similar reaction conditions discussed for compound **6**, compound **4** was reacted with HBr in acetic acid, *n*-heptanol, and K_2CO_3 in CH_2Cl_2 to produce **11**, which is the nonfluorinated structural analog of **8** with similar lipophilicity. Log *P* = 11.00. UV-vis ($\epsilon = 53\,600$ at 698 nm in THF): 543.0 (1.63×10^4), 508.0 (2.18×10^3), 414.9 (1.52×10^5), 363.9 (4.17×10^4). ^1H NMR (400 MHz, 3 mg/1 mL of CDCl_3 , δ ppm): 9.76 and 9.66 (each s, 1H for 5-H and 10-H), 8.54 (s, 1H, 20-H), 7.33 (s, 2H, 2 \times ArH), 6.90 (s, 1H, 1 \times ArH), 5.81–5.76 (m, $J = 6.8$ Hz, 1H, 3^1CH), 5.68–5.58 (m, $J = 10.9$, 2H, $\text{N}-\text{CH}_2\text{Ar}$), 5.44 (d, 2H), 3.85 (s, 4H), 3.71–3.65 (m, 4H, 8^1CH_2 and 3^1OCH_2), 3.5 (s, 3H, $17^2\text{CO}_2\text{CH}_3$), 3.50 (s, 2H), 3.31 (s, 3H, 7CH_3), 3.20 (s, 4H), 2.32 (s, 11H), 2.17 (s, 9H), 2.06 (dd, 4H), 1.69 (t, $J = 7.3$ Hz, 5H), 1.53 (s, 20H), 1.10 (t, $J = 6.8$ Hz, 2H), 0.778 (m, 4H), -0.015 (br s, 1H, 2 \times NH). Mass calculated for $\text{C}_{50}\text{H}_{61}\text{N}_5\text{O}_5$, 811.47; found, 835.5 (M + Na). HRMS calculated, 812.4751; found, 812.4746.

Purpurin-18-N-butylimide (12). Compound **1** (120 mg, 0.21 mmol) was reacted with 1 mL of *n*-butylamine (30.7 mg, 0.42 mmol) while stirring at RT in 10 mL of CH_2Cl_2 for ~ 24 h under

N_2 gas. During this time, the long wavelength absorption shifted from 699 to 666 nm. The solvent was removed and hexane was added to the dried reaction mixture, and after 2 h in the freezer, the recovered **1** was collected via filtration and the residue was washed with excess hexane. The crystals were transferred back to the reaction flask, dissolved in 10 mL of $\text{CH}_2\text{Cl}_2/\text{THF}$ (1:1), and treated with diazomethane. The intermediate were cyclized to the corresponding cyclic imide on reacting with a catalytic amount of KOH/MeOH solution for 4–5 min with vigorous stirring, and the reaction was monitored by UV-vis spectroscopy (appearance of a new peak at 706 nm). The reaction mixture was washed with 2% acetic acid in water to neutralize the KOH and washed again with water (3 \times 250 mL). The solvent was removed and purified on a silica column using a 3% MeOH in CH_2Cl_2 as an eluent (yield: 111 mg, 84.7%). UV-vis ($\epsilon = 58\,000$ at 706 nm in THF): 549.0 (2.51×10^4), 510.9 (6.33×10^3), 419.0 (1.75×10^5), 368.0 (6.05×10^4). ^1H NMR (400 MHz, 3 mg/1 mL of CDCl_3 , δ ppm): 9.47 (s, 1H, 10H), 9.23 (s, 1H, 5H), 8.55 (s, 1H, 20H), 7.82 (dd, $J = 18.0$, 11.7, 1H $3^1\text{CH}=\text{CH}_2$), 6.24 (d, $J = 18.0$, 1H, $3^1\text{CH}=\text{CH}_2$), 6.10 (d, $J = 11.7$, 1H, $3^1\text{CH}=\text{CH}_2$), 5.40 (m, 1H, 17^1H), 4.46 (m, 2H, $\text{NCH}_2\text{CH}_2\text{CH}_2\text{CH}_3$), 4.35 (q, $J = 7.3$, 1H, 18H), 3.76 (s, 3H, 12CH_3), 3.57 (s, 3H, $17^2\text{CO}_2\text{CH}_3$), 3.54 (q, $J = 7.8$, 2H, $8^1\text{CH}_2-\text{CH}_3$), 3.32 (s, 3H, 2CH_3), 3.06 (s, 3H, 7CH_3), 2.62–2.75 (m, 1H, 17^2CH_2), 2.30–2.50 (m, 2H, 17^1CH_2), 1.95–2.05 (m, 3H, 17^2CH_2 and $\text{NCH}_2\text{CH}_2\text{CH}_2\text{CH}_3$), 1.78 (d, $J = 7.0$, 3H, 18CH_3), 1.58–1.70 (m, 5H, $8^1\text{CH}_2\text{CH}_3$ and $\text{NCH}_2\text{CH}_2\text{CH}_2\text{CH}_3$), 1.12 (t, $J = 6.3$, 3H, $\text{NCH}_2\text{CH}_2\text{CH}_2\text{CH}_3$), -0.18 (br s, 1H, NH), -0.28 (br s, 1H, NH).¹⁸

3-Devinyl-3-[1-3,5-bis(dimethyl)benzyl]ethyl-purpurin-18-N-butylimide (13). Further reaction of **12** with HBr/acetic acid followed by addition of commercially available 3,5-dimethylbenzyl alcohol with K_2CO_3 and CH_2Cl_2 gave the corresponding *N*-butyl derivative **13**. The crude product was purified on preparative silica plate using 80:20 hexane/ethyl acetate. Each of these nonfluorinated analogs maintained a Log *P* value of 9.43. UV-vis ($\epsilon = 53\,600$ at 698 nm in THF): 639.0 (8.08×10^3), 543.0 (2.10×10^4), 507.0 (8.37×10^3), 478.0 (5.20×10^3), 415.1 (1.46×10^5), 364.0 (4.97×10^4). ^1H NMR (400 MHz, 3 mg/1 mL of CDCl_3 , δ ppm): 9.79 and 9.63 (each s, 1H, for 10H and 5H), 8.60 (s, 1H, for 20H), 7.79 (s, 1H, ArH), 6.96 (m, 2H, 2 \times ArH), 5.91 (m, 1H, 3^1H), 5.44 (m, 1H, 17H), 4.57 (s, 2H, OCH_2Ar), 4.49 (t, $J = 7.8$ Hz, 2H, $\text{N}-\text{CH}_2\text{C}_3\text{H}_7$), 4.39 (m, 1H, 18H), 3.82 (s, 3H, 12CH_3), 3.66 (q, $J = 7.6$ Hz, 2H, 8^1CH_2), 3.58 (s, 3H, $17^2\text{CO}_2\text{CH}_3$), 3.34 (s, 3H, 7CH_3), 3.12 (s, 3H, 2CH_3), 2.70 (m, 1H, 1 \times 17^2H), 2.46 (m, 1H, 1 \times 17^2H), 2.20–2.40 (m, 1H, 1 \times 17^1H), 2.25 (s, 6H, 2 \times Ar- CH_3), 2.12 (d, $J = 6.4$ Hz, 3H, 3^2CH_3), 2.00–2.05 (m, 3H, 1 \times 17^2H and $\text{NCH}_2\text{CH}_2\text{CH}_2\text{CH}_3$), 1.80 (d, $J = 6.8$, 3H, 8CH_3), 1.62–1.70 (m, 5H, 8^2CH_3 and $\text{N}-\text{CH}_2\text{CH}_2\text{CH}_2\text{CH}_3$), 1.12 (t, $J = 7.4$ Hz, 3H, $\text{N}-\text{CH}_2\text{CH}_2\text{CH}_2\text{CH}_3$), -0.09 (br s, 1H, NH), -0.14 (br s, 1H, NH). Mass calculated for $\text{C}_{47}\text{H}_{55}\text{N}_5\text{O}_5$, 769.42; found, 769/770 (M). HRMS calculated, 769.4209; found, 789.4234.

3-Devinyl-3-[1-3,5-bis(trifluoromethyl)benzyl]ethyl-purpurin-18-N-butylimide (14). Compound **12** (111 mg, 0.18 mmol) was reacted with ~ 2.5 mL of 30% HBr in acetic acid for ~ 1.5 h. The excess acetic acid was removed via high vacuum (~ 45 min). To the dry residue was added the commercially available 3,5-bis-(trifluoromethyl) benzyl alcohol (~ 400 mg, 1.6 mmol), 28 mg of anhydrous K_2CO_3 , and ~ 3 mL of CH_2Cl_2 . The reaction was stirred at RT under argon for ~ 3 h. At completion (shift from 708 \rightarrow 701 nm), the reaction mixture was washed with water and CH_2Cl_2 , and the organic layer was collected, dried over Na_2SO_4 , and filtered. The filtrate was rotavaporated to dryness, and the crude product was purified on analytical silica prep plates using the 1.5% MeOH in CH_2Cl_2 solvent system (yield: 13.8 mg, 10%). Log *P* = 10.91. UV-vis ($\epsilon = 58\,000$ at 700 nm in THF): 642.0 (7.66×10^3), 543.0 (2.16×10^4), 507.0 (8.19×10^3), 479.1 (4.75×10^3), 415.1 (1.51×10^5), 365.0 (5.21×10^4). ^1H NMR (400 MHz, 3 mg/1 mL of CDCl_3 , δ ppm): 9.73 and 9.68 (each s, 1H, for 10H and 5H), 8.60 (s, 1H, for 20H), 7.85 (s, 2H, 2 \times ArH), 7.81 (s, 1H, ArH), 5.96 (q, $J = 6.8$ Hz, 1H, 3^1H), 5.43 (d, $J = 8.0$ Hz, 1H, 17H), 4.79 (s, 2H, $\text{O}-\text{CH}_2\text{Ar}$), 4.48 (t, $J = 7.8$ Hz, 2H, $\text{N}-\text{CH}_2\text{C}_3\text{H}_7$), 4.38 (q, $J = 7.2$ Hz, 1H, 18H), 3.86 (s, 3H, 12CH_3), 3.69 (q, $J = 7.6$ Hz, 2H,

8^1CH_2), 3.57 (s, 3H, $17^2\text{CO}_2\text{CH}_3$), 3.10 (s, 3H, 7CH_3), 2.68 (m, 1H, $1 \times 17^2\text{H}$), 2.44 (m, 1H, $1 \times 17^1\text{H}$), 2.32 (m, $1 \times 17^1\text{H}$), 2.21 (d, $J = 6.4$ Hz, 3H, 3^2CH_3), 1.99 (m, $J = 5.4$ Hz, 3H, $\text{N}-\text{CH}_2\text{CH}_2-\text{CH}_2\text{CH}_3$ and $1 \times 17^2\text{H}$), 1.78 (d, $J = 6.8$ Hz, 3H, 18CH_3), 1.66 (m, 5H, $\text{N}-\text{CH}_2\text{CH}_2\text{CH}_2\text{CH}_3$ and 8^2CH_3), 1.11 (t, $J = 7.4$ Hz, 3H, $\text{N}-\text{CH}_2\text{CH}_2\text{CH}_2\text{CH}_3$), -0.18 (br s, 1H, NH), -0.21 (br s, 1H, NH). ^{19}F NMR (400 MHz, 3 mg/1 mL of CDCl_3 , in reference to TFA, δ ppm): 12.60. Mass calculated for $\text{C}_{47}\text{H}_{49}\text{N}_5\text{O}_5\text{F}_6$, 877.36; found, 879 (M + 2). HRMS calculated (M + 1), 878.3716; found, 878.3742 (M + 1).

3-Devinyl-3-(1'-butoxyethyl)-purpurin-18-N-3,5-bis(trifluoromethyl)benzyl-17-aminobenzyl-DTPA-imide (24). PS 8 (130 mg, 0.15 mmol) was dried under high vacuum, dissolved in dry degassed THF (40 mL), and stirred under N_2 gas. Upon addition of LiOH solution (with minimal MeOH added to the reaction mixture), the mixture changed from a dark/purple hue to green. After ~ 3 h, the reaction was stopped and washed with CH_2Cl_2 . The organic layer was collected, dried over Na_2SO_4 , filtered, and evaporated to dryness (yield: 130 mg, 100%). To this crude product (130 mg, 0.15 mmol) was added amino-DTPA *t*-butyl protected (170 mg), 20 mg of 4-(dimethylamino)pyridine (DMAP), and 49 mg of 1,3-dicyclohexylcarbodiimide (DCC) in ~ 4 mL of dry CH_2Cl_2 . The reaction was stirred under N_2 gas for ~ 24 h, and excess water (1–2 mL) was added to decompose DCC. The organic layer was collected, dried over Na_2SO_4 , filtered, and evaporated to dryness. Excess CH_2Cl_2 was added to crystallize out DCC impurity (urea) that was later removed by filtration. The product was purified on silica prep plates using 8% MeOH in CH_2Cl_2 and then on an Alumina III column, first eluting with CH_2Cl_2 , followed by ethyl acetate/ CH_2Cl_2 (1:9). The final solvent system of ethyl acetate/ CH_2Cl_2 (1:3) yielded 105 mg of 23 (mass calculated for $\text{C}_87\text{H}_{115}\text{N}_9\text{O}_{14}\text{F}_6$, 1624.89; found, 1647.6 (M + Na + H)). For deprotection, a small amount of concentrated trifluoroacetic acid (TFA) was added to the DTPA-protected compound (~ 9 mg) and stirred at RT for ~ 3 h. TFA was removed under high vacuum. The residue was dissolved in 3 mL Na_2HPO_4 and then 3 mL NaH_2PO_4 , which yielded 24 formulated in a water-based solution at a pH of ~ 7.4 . Log *P* = -6.45 . UV-vis ($\epsilon = 41,181$ at 711 in H_2O): 659.1 (1.19×10^4), 550.0 (2.24×10^4), 513.0 (7.22×10^3), 481.1 (5.78×10^3), 418.9 (1.06×10^5), 363.9 (7.08×10^4). HRMS calculated, 1343.5337; found, 1343.5350.

Bacteriopurpurinimides. Synthesis of Bacteriopurpurin-18 Methyl Ester (15). *Rb. sphaeroides* (~ 1.5 kg) and ~ 3000 mL of *N*-propanol were stirred overnight with a continuous flow of N_2 gas bubbled through the mixture. The bacterial sludge was filtered through a buchner funnel, and the blackish-blue/green filtrate was collected (peak absorbance at 776 nm in *N*-propanol). A KOH solution was added to the filtrate. With O_2 bubbling through the solution, the reaction was stirred for ~ 1 h at RT. The reaction was complete when a wavelength absorption shift occurred from 776 to 768 nm. At this point, the mixture was red; however, when transferring to the ice + water solution, the mixture turned bluish-green. While stirring, 5% H_2SO_4 was added dropwise until the mixture reached a pH in the range of 2–3 (changed back to dark red hue). The mixture was washed with water and CH_2Cl_2 , and the organic layer was collected, dried over Na_2SO_4 , and filtered. The filtrate was rotovapped to dryness and refluxed in THF for ~ 30 min until a peak at ~ 815 nm was noticeable. Hexane was added to the residue, and the solid was collected via Buchner funnel filtration. The filtrate mainly containing the carotene analogs was discarded, and the solid, isolated as a carboxylic acid analog, was treated with diazomethane and converted into the methyl ester. The crude material was purified on a silica column using 2% acetone in CH_2Cl_2 (yield: ~ 2.2 g). UV-vis (in CH_2Cl_2): 364 nm ($\epsilon 8.91 \times 10^4$), 412 nm ($\epsilon 5.36 \times 10^4$), 545 nm ($\epsilon 3.4 \times 10^4$), 815 nm ($\epsilon 5.53 \times 10^4$). ^1H NMR (400 MHz, 3 mg/1 mL CDCl_3 , δ ppm): 9.21 (s, 1H, 5-H), 8.78 (s, 1H, 10-H), 8.62 (s, 1H, 20-H), 5.13 (m, 1H, 17-H), 4.30 (m, 2H, 1H for 7-H, 1H for 18-H), 4.08 (m, 1H, 8-H), 3.63 (s, 3H, $12-\text{CH}_3$), 3.57 (s, 3H, $-\text{COOCH}_3$), 3.52 (s, 3H, $2-\text{CH}_3$), 3.15 (s, 3H, CH_3C), 2.70 (m, 1H, $-\text{CHHCH}_2\text{COOCH}_3$), 2.42 (m, 2H, $8-\text{CH}_2\text{CH}_3$), 2.35 (m, 1H, $-\text{CHHCH}_2\text{COOCH}_3$), 2.00

(m, 2H, $-\text{CH}_2\text{CH}_2\text{COOCH}_3$), 1.80 (d, $J = 7.17$ Hz, 3H, $7-\text{CH}_3$), 1.70 (d, $J = 6.82$ Hz, 3H, $18-\text{CH}_3$), 1.1 (t, $J = 6.46$ Hz, 3H, $8-\text{CH}_2\text{CH}_3$), -0.03 (s, 1H, NH), -0.65 (s, 1H, NH). Anal. Calcd for $\text{C}_{34}\text{H}_{36}\text{N}_4\text{O}_6\text{H}_2\text{O}$: C, 66.42; H, 6.24; N, 9.12. Found: C, 66.30; H, 5.90; N, 8.99. Mass (*m/e*) calcd for $\text{C}_{34}\text{H}_{36}\text{N}_4\text{O}_6$, 596.3; found, 596.8 (M + 1). HRMS calcd, 596.2635; found, 596.2615.

Bacteriopurpurin-18-N-3,5-bis(trifluoromethyl)benzylimide Methyl Ester (16). Compound 15 (250 mg, 0.42 mmol) and 3,5-bis(trifluoromethyl)benzyl amine (3 g, 0.012 mol) were refluxed in 25 mL of dry benzene under N_2 gas for ~ 24 h. According to TLC (3% MeOH in CH_2Cl_2 on silica), there was a mixture of two compounds, the desired 16 and a byproduct (3-acetyl-3-[1'-3,5-bis(trifluoromethyl)benzyl]ethyl-bacteriopurpurin-18-N-3,5-bis(trifluoromethyl)benzyl imide). The reaction was stopped and washed with water and CH_2Cl_2 . The organic layer was collected, dried over Na_2SO_4 , and concentrated under vacuum. As a means to convert everything to the desired product, the crude material was dissolved in CH_2Cl_2 and treated with dilute HCl (the reaction was monitored by UV-vis). The reaction yielded a single peak at 826 nm, converting the majority of product to 16. Upon completion, the reaction was immediately washed with water and CH_2Cl_2 (3 \times), and the organic layer was collected, dried over Na_2SO_4 , and concentrated under vacuum. The crude material was purified on silica prep plates in 1% acetone in CH_2Cl_2 (yield: 245 mg, 71%). UV-vis ($\epsilon = 59,500$ at 820 in THF): 544.9 (3.19×10^4), 414.9 (3.87×10^4), 363.9 (7.45×10^4). ^1H NMR (400 MHz, 3 mg/1 mL of CDCl_3 , δ ppm): 9.20 (s, 1H, 5-H), 8.80 (s, 1H, 10-H), 8.60 (s, 1H, 20-H), 8.19 (s, 2H, Ar-H), 7.80 (s, 1H, Ar-H), 5.74 (s, 2H, NCH_2Ar), 5.25 (m, 1H, 17-H), 4.22–4.32 (m, 2H, 7-H and 18-H), 4.05–4.15 (m, 1H, 8-H), 3.70 (s, 3H, $12-\text{CH}_3$), 3.55 (s, 3H, $17^2-\text{CO}_2\text{CH}_3$), 3.54 (s, 3H, $2-\text{CH}_3$), 3.17 (s, 3H, $3-\text{COCH}_3$), 2.60–2.70 (m, 1H, $1 \times 17^1\text{H}$), 2.43 (m, 3H, 8^1CH_2 and $1 \times 17^1\text{H}$), 2.00–2.10 (m, 1H, $1 \times 17^2\text{H}$), 1.85–1.95 (m, 1H, $1 \times 17^2\text{H}$), 1.81 (d, $J = 5.8$, 3H, $7-\text{CH}_3$), 1.72 (d, $J = 6.9$, 3H, $18-\text{CH}_3$), 1.10 (t, $J = 7.0$, 3H, 8^2CH_3), -0.35 (br s, 1H, NH), -0.61 (br s, 1H, NH). Mass calculated for $\text{C}_{43}\text{H}_{41}\text{N}_5\text{O}_5\text{F}_6$, 821.30; found, 844.4 (M + Na). HRMS calculated, 821.3012; found, 821.3007.

3-Deacetyl-3-(1'-hydroethyl)-bacteriopurpurin-18-N-3,5-bis(trifluoro-methyl)benzylimide (17). Compound 16 (31 mg, 0.38 mmol) was initially dissolved in ~ 20 –25 mL of dry CH_2Cl_2 and MeOH (~ 5 –10 mL). In small increments, a total of 60 mg of dry NaBH_4 was added, and the reaction mixture was stirred for 30 min. After completion of the reaction (monitored by analytical TLC and spectrophotometry), the contents were transferred to a beaker containing ice + water. A 2% aqueous acetic acid solution was slowly added to the reaction mixture until the solution became neutral (pH = ~ 7). The mixture was then washed with water (100 mL), the organic layer was concentrated under vacuum, and the residue was purified on silica prep plates in 2% acetone in CH_2Cl_2 (yield: 25 mg, 80.6%). UV-vis ($\epsilon = 40,530$ at 778 in THF): 537.0 (3.94×10^4), 504.0 (3.94×10^3), 469.0 (3.01×10^3), 416.9 (4.47×10^4), 367.0 (9.94×10^4), 347.0 (4.45×10^4). ^1H NMR (400 MHz, 3 mg/1 mL of CDCl_3 , δ ppm): 8.80 (s, $1/2\text{H}$, $1/2\text{5-H}$), 8.78 (s, $1/2\text{H}$, $1/2\text{5-H}$), 8.56 (s, 1H, 10-H), 8.29 (s, 1H, 20-H), 8.19 (s, 2H, Ar-H), 7.80 (s, 1H, Ar-H), 6.18 (q, $J = 6.6$, 1H, 3^1H), 5.72 (m, 2H, NCH_2Ar), 5.19 (m, 1H, 17-H), 4.12–4.22 (m, 2H, 7-H and 18-H), 3.95–4.02 (m, 1H, 8-H), 3.59 (s, 3H, $12-\text{CH}_3$), 3.56 (s, $3/2\text{H}$, $1/2\text{17}^2\text{CO}_2\text{CH}_3$), 3.55 (s, $3/2\text{H}$, $1/2\text{17}^2\text{CO}_2\text{CH}_3$), 3.24 (s, 3H, $2-\text{CH}_3$), 2.60–2.70 (m, 2H, $2 \times 17^1\text{H}$), 2.24–2.40 (m, 3H, 8^1CH_2 and $1 \times 17^2\text{H}$), 2.05 (d, $J = 6.8$, 3H, 3^1CH_3), 1.85–1.95 (m, 1H, $1 \times 17^2\text{H}$), 1.78 (dd, $J = 3.0, 3.5$, 3H, $7-\text{CH}_3$), 1.68 (m, 3H, $18-\text{CH}_3$), 1.09 (t, $J = 6.6$, 3H, 8^2CH_3), 0.28 (br s, 1H, NH); -0.11 (br s, 1H, NH). HRMS calculated, 823.3168; found, 823.3173.

3-Deacetyl-3-(1'-methoxyethyl)-bacteriopurpurin-18-N-3,5-bis(trifluoro-methyl)benzylimide (18). A similar procedure as described for 7–10 was followed for compounds 18–21, except instead of using HBr/acetic acid, the HBr gas was used for the preparation of the intermediate bromo derivative (under HBr/acetic acid conditions, the bacteriopurpurinimides were found to be unstable). Compound 17 (45 mg, 0.055 mmol) was dissolved in ~ 30 mL of dry CH_2Cl_2 . All air was removed from the reaction

flask and flushed with argon. Then under completely dry conditions, HBr gas was passed through a needle and submerged into the solution for ~20 s. While stirring for ~10 min, there appeared to be a visible change from dark green to a purple hue of the solution. The reaction mixture was then concentrated under high vacuum for ~1 h, which yielded a dark purple residue. To the residue was added ~30 mL of dry CH₂Cl₂, 90 mg of dry K₂CO₃, and 1.5 mL of *n*-methanol, which was stirred under N₂ gas for ~30 min. Upon completion, the contents were transferred to a beaker containing ice + water, and the pH was adjusted to 2–2.5 by adding aqueous acetic acid. After additional washes with water and CH₂Cl₂ (3×), the organic layer was collected, dried over Na₂SO₄, and concentrated under vacuum at room temperature to yield a dark purple crude material. The crude material was purified on silica prep plates using a hexane/ethyl acetate (80:20) solvent system. The pure compound exhibited a characteristic absorption peak at 783 nm in CH₂Cl₂ (yield: 23.8 mg, 51.7%). Log *P* = 8.82. UV–vis (ε = 40 530 at 784 in THF): 538.0 (3.91 × 10⁴), 503.0 (5.63 × 10³), 417.1 (5.49 × 10⁴), 367.0 (1.01 × 10⁵), 346.0 (4.93 × 10⁴). ¹H NMR (400 MHz, 3 mg/1 mL of CDCl₃, δ ppm): 8.76 (s, 1/2H, 1/25-H), 8.72 (s, 1/2H, 1/25-H), 8.56 (s, 1H, 10-H), 8.29 (s, 1H, 20-H), 8.19 (s, 2H, Ar–H), 7.78 (s, 1H, Ar–H), 5.72 (m, 2H, NCH₂Ar), 5.54–5.60 (m, 1H, 3¹H), 5.19 (m, 1H, 17-H), 4.12–4.22 (m, 2H, 7-H and 18-H), 3.95–4.02 (m, 1H, 8-H), 3.60 (s, 3H, 3¹OCH₃), 3.55 (s, 3H, 12-CH₃), 3.50 (s, 3H, 17²CO₂CH₃), 3.22 (s, 3H, 2-CH₃), 2.58–2.68 (m, 1H, 1 × 17¹H), 2.24–2.40 (m, 3H, 8¹CH₂ and 1 × 17¹H), 2.00–2.10 (m, 1H, 1 × 17²H), 1.98 (dd, *J* = 2.5, 5.0, 3H, 3¹CH₃), 1.85–1.95 (m, 1H, 1 × 17²H), 1.78 (t, *J* = 8.0, 3H, 7-CH₃), 1.68 (d, *J* = 7.6, 3H, 18-CH₃), 1.12 (t, *J* = 6.6, 3H, 8²CH₃), 0.30 (br s, 1H, NH), –0.09 (br s, 1H, NH). ¹⁹F NMR (400 MHz, 3 mg/1 mL of CDCl₃, in reference to TFA, δ ppm): 13.14. Mass calculated for C₄₄H₄₅N₅O₅F₆, 837.33; found, 860.4 (M + Na). HRMS calculated (M + 1), 838.3403; found, 838.3467.

3-Deacetyl-3-(1¹-butoxyethyl)-bacteriopurpurin-18-N-3,5-bis(trifluoro-methyl)benzylimide (19). A similar procedure as described for **18** was followed. Compound **17** (24.6 mg, 0.030 mmol) was dissolved in ~15 mL of dry CH₂Cl₂. All air was removed from the reaction flask and flushed with argon. Then under completely dry conditions, HBr gas was passed through a needle and submerged into the solution for ~20 s. While stirring for ~5 min, there appeared to be a visible change from dark green to a purple hue of the solution. The reaction mixture was then concentrated under high vacuum for ~1 h, which yielded a dark purple residue. To the residue was added ~15–20 mL of dry CH₂Cl₂, 50 mg of dry K₂CO₃, and 1 mL of *n*-butanol, which was stirred under N₂ gas for ~35 min. Upon completion, the contents were transferred to a beaker containing ice water, and the pH was adjusted in the range of 2–2.5. After additional washes with water and CH₂Cl₂ (3×), the organic layer was collected, dried over Na₂SO₄, and concentrated under vacuum without heat to yield a dark purple crude material. There were problems finding the best solvent system for purification. Initially the crude material was purified on silica prep plates using a 1–2% acetone in CH₂Cl₂ solvent system. After many purification steps, the desired compound was finally purified using 1.5% MeOH in CH₂Cl₂ (yield: 13.1 mg, 49.6%). Log *P* = 10.30. UV–vis (ε = 40 530 at 785 in THF): 537.9 (3.86 × 10⁴), 504.0 (5.25 × 10³), 470.0 (4.56 × 10³), 417.0 (4.44 × 10⁴), 367.1 (9.66 × 10⁴), 347.0 (4.51 × 10⁴). ¹H NMR (400 MHz, 3 mg/1 mL of CDCl₃, δ ppm, *R*-isomer): 8.78 (s, 5-H), 8.57 (s, 1H, 10-H), 8.28 (s, 1H, 20-H), 8.20 (s, 2H, Ar–H), 7.80 (s, 1H, Ar–H), 5.74 (m, 2H, NCH₂Ar), 5.65 (m, 1H, 3¹H), 5.19 (m, 1H, 17-H), 4.18 (m, 2H, 7-H and 18-H), 4.00 (m, 1H, 8-H), 3.61 (s, 4H, 12-CH₃ and 1 × 3¹(OCH₂C₃H₇)), 3.56 (s, 4H, 17²CO₂CH₃ and 1 × 3¹(OCH₂C₃H₇)), 3.22 (s, 3H, 2-CH₃), 2.64 (m, 1H, 1 × 17¹H), 2.33 (m, 3H, 2H for 8¹CH₂ and 1H for 17¹H), 2.00 (m, 1H, 1 × 17²H), 1.99 (d, *J* = 6.5, 3H, 3¹CH₃), 1.94 (m, 1H, 1 × 17²H), 1.80 (d, *J* = 6.6, 3H, 7-CH₃), 1.70 (m, 5H, 18-CH₃ and 3¹OCH₂CH₂C₂H₅), 1.27 (m, 2H, 3¹O(CH₂)₂CH₂CH₃), 1.11 (m, 3H, 8²CH₃), 0.89 (m, 3H, 3-CH₃CH(O(CH₂)₃CH₃)), 0.35 (br s, 1H, NH), –0.05 (br s, 1H, NH). *S*-isomer: 8.83 (s, 5-H), 8.58 (s, 1H, 10-H), 8.28 (s, 1H, 20-H), 8.20 (s, 2H, Ar–H), 7.80 (s, 1H, Ar–H), 5.76 (m, 2H,

NCH₂Ar), 5.64 (m, 1H, 3¹H), 5.20 (m, 1H, 17-H), 4.19 (m, 2H, 7-H and 18-H), 4.00 (m, 1H, 8-H), 3.61 (s, 4H, 12-CH₃ and 1 × 3¹(OCH₂C₃H₇)), 3.56 (s, 4H, 17²CO₂CH₃ and 1 × 3¹(OCH₂C₃H₇)), 3.22 (s, 3H, 2-CH₃), 2.65 (m, 1H, 1 × 17¹H), 2.33 (m, 3H, 2H for 8¹CH₂ and 1H for 17¹H), 2.00 (m, 1H, 1 × 17²H), 1.99 (d, *J* = 6.5, 3H, 3¹CH₃), 1.95 (m, 1H, 1 × 17²H), 1.79 (d, *J* = 6.6, 3H, 7-CH₃), 1.70 (m, 5H, 18-CH₃ and 3¹OCH₂CH₂C₂H₅), 1.28 (m, 2H, 3¹O(CH₂)₂CH₂CH₃), 1.12 (m, 3H, 8²CH₃), 0.88 (m, 3H, 3-CH₃CH(O(CH₂)₃CH₃)), 0.36 (br s, 1H, NH), –0.04 (br s, 1H, NH). Mass calculated for C₄₇H₅₁O₅F₆, 879.38; found, 902.3 (M + Na). HRMS calculated, 879.3799; found, 879.3798.

3-Deacetyl-3-(1¹-heptyloxyethyl)-bacteriopurpurin-18-N-3,5-bis(trifluoro-methyl)benzylimide (20). A similar procedure as described for **18** was followed. Compound **17** (45 mg, 0.055 mmol) was dissolved in ~30 mL of dry CH₂Cl₂. All air was removed from the reaction flask and flushed with argon. Then under completely dry conditions, HBr gas was passed through a needle and submerged into the solution for ~20 s. While stirring for ~10 min, there appeared to be a visible change from dark green to a purple hue of the solution. The reaction mixture was then concentrated under high vacuum for ~1 h, which yielded a dark purple residue. To the residue was added ~30 mL dry CH₂Cl₂, 90 mg anhydrous K₂CO₃ and 1.5 mL *n*-heptanol which was stirred under N₂ gas for ~30 min. Upon completion, the contents were transferred to a beaker containing ice water, and the pH was adjusted to 2–2.5. After additional washes with water and CH₂Cl₂ (6×), the organic layer was collected, dried over Na₂SO₄, and concentrated under vacuum without heat to yield a dark purple crude material. The crude material was purified on silica prep plates using a hexane/ethyl acetate (80:20) solvent system. The pure compound exhibited a characteristic absorption peak at 783 nm in CH₂Cl₂ (yield: 35.9 mg, 70.8%). Log *P* = 11.83. UV–vis (ε = 40 530 at 784 in THF): 537 (3.90 × 10⁴), 505.0 (5.49 × 10³), 472.0 (5.23 × 10³), 417.1 (4.59 × 10⁴), 367.0 (9.79 × 10⁴), 346.9 (4.67 × 10⁴). ¹H NMR (400 MHz, 3 mg/1 mL of CDCl₃, δ ppm): 8.82 (s, 1/2H, 1/25-H), 8.78 (s, 1/2H, 1/25-H), 8.56 (s, 1H, 10-H), 8.27 (s, 1H, 20-H), 8.19 (s, 2H, Ar–H), 7.78 (s, 1H, Ar–H), 5.72 (m, 2H, N–CH₂Ar), 5.63 (m, 1H, 3¹H), 5.17 (m, 1H, 17-H), 4.10–4.20 (m, 2H, 7-H and 18-H), 3.94–4.00 (m, 1H, 8-H), 3.60 (s, 4H, 12-CH₃ and 1 × 3¹OCH₂C₃H₇), 3.54 (s, 4H, CO₂CH₃ and 1 × 3¹OCH₂C₆H₁₃), 3.20 (s, 3/2H, 1/2-2-CH₃), 3.21 (s, 3/2H, 1/2-2-CH₃), 2.55–2.65 (m, 1H, 1 × 17¹H), 2.24–2.40 (m, 3H, 8¹CH₂ and 1 × 17¹H), 2.00–2.10 (m, 1H, 1 × 17²H), 1.98 (d, *J* = 6.8, 3H, 3¹CH₃), 1.85–1.95 (m, 1H, 1 × 17²H), 1.78 (t, *J* = 7.5, 3H, 7-CH₃), 1.65–1.72 (m, 5H, 18-CH₃ and 3¹OCH₂CH₂C₅H₁₁), 1.20–1.36 (m, 8H, 3¹O(CH₂)₂(CH₂)₄CH₃), 1.05–1.15 (m, 3H, 8²CH₃), 0.78–0.82 (m, 3H, 3¹O(CH₂)₆CH₃), 0.35 (br s, 1H, NH), –0.06 (br s, 1H, NH). ¹⁹F NMR (400 MHz, 3 mg/1 mL of CDCl₃, in reference to TFA, δ ppm): 13.14. Mass calculated for C₅₀H₅₇N₅O₅F₆, 921.43; found, 944.5 (M + Na). HRMS calculated, 921.4264; found, 921.4259.

3-Deacetyl-3-(1¹-dodecyloxyethyl)-bacteriopurpurin-18-N-3,5-bis(trifluoro-methyl)benzylimide (21). A similar procedure as described for **18** was followed. Compound **17** (45 mg, 0.055 mmol) was dissolved in ~30 mL of dry CH₂Cl₂. All air was removed from the reaction flask and flushed with argon. Then under completely dry conditions, HBr gas was passed through a needle and submerged into the solution for ~20 s. While stirring for ~10 min, there appeared to be a visible change from dark green to a purple hue of the solution. The reaction mixture was then concentrated under high vacuum for ~1 h, which yielded a dark purple residue. To the residue was added ~30 mL of dry CH₂Cl₂, 90 mg of dry K₂CO₃, and 1.5 mL of *n*-dodecanol, which was stirred under N₂ gas for ~30 min. Upon completion, the contents were transferred to a beaker containing ice + water and the pH was adjusted to 2–2.5, and the contents were additionally washed with water, CH₂Cl₂ (6×), and ethyl ether (3×). The residue remained oily in nature, so the sample was run on a silica column first with CH₂Cl₂ so that the excess dodecanol would be removed and then with hexane/ethyl acetate (80:20) as a means to collect the sample. The eluent was collected, dried over Na₂SO₄, and concentrated under vacuum without heat to yield a dark purple crude material. Again the

material was purified on a silica prep plate using the same solvent system as mentioned above to yield the desired compound (yield: 25.8 mg, 47.3%). Log *P* = 14.38. UV-vis (ϵ = 40 530 at 785 in THF): 537.1 (3.97×10^4), 506.0 (6.06×10^3), 470.0 (5.43×10^3), 417.0 (4.91×10^4), 367.0 (9.97×10^4), 348.0 (4.83×10^4). ¹H NMR (400 MHz, 3 mg/1 mL of CDCl₃, δ ppm): 8.82 (s, ¹/₂H, ¹/₂5-H), 8.78 (s, ¹/₂H, ¹/₂5-H), 8.56 (s, 1H, 10-H), 8.27 (s, 1H, 20-H), 8.19 (s, 2H, Ar-H), 7.78 (s, 1H, Ar-H), 5.72 (m, 2H, NCH₂-Ar), 5.63 (m, 1H, 3¹H), 5.17 (m, 1H, 17-H), 4.10–4.20 (m, 2H, 7-H and 18-H), 3.94–4.00 (m, 1H, 8-H), 3.60 (s, 4H, 12-CH₃ and 3¹OCH₂C₃H₇), 3.54 (s, 4H, CO₂CH₃ and 3¹OCH₂C₆H₁₃), 3.20 (s, ³/₂H, ¹/₂2-CH₃), 3.21 (s, ³/₂H, ¹/₂2-CH₃), 2.55–2.65 (m, 1H, 1 \times 17¹H), 2.24–2.40 (m, 3H, 8¹CH₂ and 1 \times 17¹H), 2.00–2.10 (m, 1H, 1 \times 17²H), 1.98 (d, *J* = 6.8, 3H, 3¹CH₃), 1.85–1.95 (m, 1H, 1 \times 17²H), 1.78 (t, *J* = 7.5, 3H, 7-CH₃), 1.65–1.72 (m, 5H, 18-CH₃ and 3¹OCH₂CH₂C₅H₁₁), 1.20–1.36 (m, 8H, 3¹O(CH₂)₂(CH₂)₄-CH₃), 1.05–1.15 (m, 3H, 8²CH₂CH₃), 0.78–0.82 (m, 3H, 3-CH₃-CH(O(CH₂)₆CH₃)), 0.35 (br s, 1H, NH), –0.06 (br s, 1H, NH). Mass calculated for C₅₅H₆₇N₉O₅F₆, 991.50; found, 1014.7 (M + Na) and 1030.0 (M + K). HRMS calculated (M + 1), 992.5124; found, 992.5168 (M + 1).

DTPA Conjugate of Bacteriopurpurinimide (26). Compound **19** (60.0 mg, 0.068 mmol) was taken in a flask (100 mL) and dissolved in an acetonitrile–methanol mixture (20:5 mL). The resultant mixture was stirred, degassed three times, and filled with N₂ gas. To this mixture LiOH (500.0 mg) in H₂O (20 mL) was added, and the mixture was degassed again and kept for vigorous stirring for 4 h at RT under a N₂ atmosphere. The mixture was partially concentrated, acidified with dilute acetic acid, and extracted with dichloromethane (3 \times 50 mL). Organic layers were separated, combined, washed with water (3 \times 50 mL), dried over sodium sulfate, and concentrated. The crude acid **25** thus obtained was dried under vacuum for several hours to remove the traces of water and acetic acid and then used directly to couple with aminobenzyl–DTPA. The above crude acid was dissolved in dry CH₂Cl₂ (30 mL) and 4-aminobenzyl-(CO₂*t*-Bu)–DTPA (108.0 mg, 0.136 mmol), EDCI (26.2 mg, 0.136 mmol), and DMAP (16.7 mg, 0.136 mmol) were added to it. The resultant mixture was stirred at room temperature for 16 h under a N₂ atmosphere, diluted with CH₂Cl₂ (100 mL), and washed with brine (50 mL). The organic layer was separated, dried over sodium sulfate, and concentrated. The crude product was purified on a silica gel column using MeOH/CH₂Cl₂ (5–10%) as eluent to give product **26** (yield: 50.0 mg; 45%). ¹H NMR (400 MHz, CDCl₃): δ 8.81 (s, 1H, meso-H), 8.54 (s, 1H, meso-H), 8.25 (s, 1H, meso-H), 8.14 (s, 2H, bis-CF₃–C₆H₃), 7.95 (s, 1H, NH), 7.77 (m, 2H, bis-CF₃–C₆H₃ and NH), 7.44 (d, 2H, Ph-DTPA, *J* = 7.6 Hz), 7.16 (d, 2H, Ph-DTPA, *J* = 7.6 Hz), 5.83 (d, 1H, benzylic CH₂, *J* = 14.8 Hz), 5.73 (d, 1H, benzylic CH₂, *J* = 14.4 Hz), 5.61 (m, 1H, CH₃CHObutyl), 5.17 (d, 1H, H-17, *J* = 8.4 Hz), 4.29 (m, 1H, H-8), 4.14 (m, 1H, H-18), 3.96 (m 1H, H-7), 3.59 (m, 4H, OCH₂butyl and CH₂-DTPA), 3.55 (m, 2H, CH₂-DTPA), 3.44 (ss, 3H, ring-CH₃), 3.40 (m, 4H, 2CH₂-DTPA), 3.32 (m, 2H, CH₂-DTPA), 3.17 (s, 3H, ring-CH₃), 3.06 (m, 1H, CH-DTPA), 2.79–2.73 (m, 8H, 4CH₂-DTPA), 2.56–2.47 (m, 2H, 17²-CH₂), 2.34–2.29 (m, 2H, 8-CH₂CH₃), 2.05 (m, 1H, 17¹-CH₂), 1.99 (d, 3H, CH₃CHObutyl, *J* = 6.4 Hz), 1.93 (m, 1H, 17¹-CH₂), 1.79 (d, 3H, 18-CH₃, *J* = 6.4 Hz), 1.67 (d, 3H, 7-CH₃, *J* = 7.2 Hz), 1.46 (m, 4H, 2CH₂butyl), 1.42 (s, 36H, 4CO₂*t*-Bu), 1.39 (s, 9H, CO₂*t*-Bu), 1.14 (t, 3H, 8-CH₂CH₃, *J* = 7.2 Hz), 0.86 (t, 3H, CH₃-butyl, *J* = 5.2 Hz), 0.50 (br s, 1H, NH), 0.09 (br s, 1H, NH). HRMS calculated for C₈₇H₁₁₇N₉O₁₄F₆, 1625.8623; found, 1625.8646.

Methods for Determining the Photophysical Properties. The final compounds were characterized by absorbance (CARY 50 UV-Visible Spectrophotometer with Varian v2.0 software), fluorescence (Fluoromax II Fluorimeter with Thermo Galactic GRAMS/32 v4.0 software), ¹H NMR and ¹⁹F NMR (spectra obtained using a Bruker 400 MHz spectrometer; chemical shifts relative to CDCl₃ at 7.26 ppm and TFA 116.68 ppm), and mass spectrometry (analyses performed at RPCI Biopolymer Facility).

A SPEX 270M Spectrometer (Jobin Yvon) equipped with an InGaAs photodetector (Electro-Optical Systems Inc., U.S.A.) was

utilized for acquisition of ¹O₂ emission spectra. A diode pumped solid-state laser (Verdi, Coherent) at 532 nm was used to excite the photosensitizers and reference samples at room temperature (Rose Bengal purchased from Fisher Scientific, Hampton, NH). The ¹O₂ yield for Rose Bengal in MeOH solution is Q_{Δ} = 0.80.¹⁹ All samples were dissolved in MeOH solution purchased from J.T. Baker (Phillipsburg, NJ), which was used without purification. Once dissolved in MeOH, the sample was transferred into a quartz cuvette where it was placed directly in front of the entrance slit of the spectrometer, and the exciting laser beam was directed at 90 degrees relative to the collection of emission. Long-pass filters, 538AELP and 950 LP (Omega Optical, U.S.A.), were used to attenuate the excitation laser light and fluorescence from dyes as a means of studying singlet oxygen phosphorescence peaked at around 1270 nm.

Cell Culture. The RIF tumor cells grown in alpha-minimum essential medium (α -MEM; GIBCO Invitrogen Corporation), and the murine colon carcinoma (Colon-26) tumor cells grown in RPMI-1640 (GIBCO Invitrogen Corporation) with 10% FCS (BenchMark FCS Triple 0.1 μ m filtered – Gemini Bio-Products, Woodland CA), L-glutamine, and P/S/N were maintained in 5% CO₂, 95% air, and 100% humidity. The L-glutamine and P/S/N were purchased from MediaTech Cellgro, and the Trypsin/EDTA solution 1 \times sterile was purchased from Cascade Biologics. The 96-well and 6-well plates were purchased from VWR. The MTT cell viability experiments²⁰ were read using a Titertek Multiskan PLUS MKII plate reader with Multiskan Interference Filter 560 nm (Flow Laboratories, Inc.), and data were collected with the HyperTerminal Hilgraeve, Inc., program. All compounds were formulated in a 1% Tween 80/5% aqueous dextrose solution and diluted in complete medium for all in vitro experiments.

Determination of In Vitro Photosensitizing Activity. To assess the photosensitizing ability of the purpurinimides and bacteriopurpurinimides, the RIF cells were seeded in 96-well plates at a density of 5 \times 10³ cells/well in α -MEM complete media. For determining the photosensitizing ability of the water-soluble photosensitizer **24**, the colon-26 cells were seeded at 4 \times 10³ cells/well in RPMI-1640 complete media. The next day, photosensitizers were added at variable concentrations (1.25–20 μ M). After the 24 h of incubation in the dark at 37 $^{\circ}$ C, the cells were replaced with complete media and exposed to 708 nm (**7–11**) or 791 nm (**18–21**) at a dose rate of 3.2 mW/cm² at various light doses (0.5–20 J/cm²). The dye laser (375; Spectra Physics, Mt. View, CA) was excited by an argon-pumped laser tuned to emit drug-activating wavelengths. Uniform illumination was accomplished using a 200- μ m diameter quartz optical fiber fitted with a graded index refraction lens. Following illumination, the plates were incubated at 37 $^{\circ}$ C in the dark for 48 h. Appropriate dark controls at variable drug doses were also included. Following the 48 h incubation in the dark, the plates were evaluated for cell viability using the MTT assay.²⁰ At this point, 10 μ L of 4.0 mg/mL of solution of MTT dissolved in PBS (Sigma Chemical Co., St. Louis, MO) was added to each well. After the 4 h MTT incubation, the MTT + media were removed and 100 μ L of dimethyl sulfoxide was added to solubilize the formazin crystals. The PDT efficacy was measured by reading the 96-well plate on a microtiter plate reader (Miles Inc., Titertek Multiskan Plus MK II) at an absorbance of 560 nm. The results were plotted as percent survival compared with the corresponding dark (drug, no light) and light control (cells + light dose in J/cm²). Each data point represents the mean from a typical experiment with four replicate wells, and the error bars are the standard deviation from three separate experiments.

Determination of In Vivo Uptake by In Vivo Reflectance Spectroscopy (IRS). The female C3H mice 5–8 weeks of age were obtained from the NCI Jackson Laboratory. At 7–14 weeks of age the mice were inoculated s.c. with RIF (3 \times 10⁵ cells in 40 μ L) on the right posterior shoulder. The female BALB/c mice 6–8 weeks of age obtained from the NCI Clarence Reeder were used for the water soluble photosensitizer studies. At 8–14 weeks of age, the mice were inoculated s.c. with colon-26 (1 \times 10⁶ cells in 50 μ L) on the right posterior shoulder. When tumors reached \sim 7 mm³,

the mice were anesthetized using ketamine xylazine intraperitoneally. The optical power as a function of wavelength was recorded before the i.v. injection of the photosensitizer. The measurements were acquired through the use of bundle optical fibers that were positioned on the surface of the tumor plus overlying skin and normal skin. The drug at 2.5–5.0 $\mu\text{mol/kg}$ was then injected (via i.v. tail vein), and the absorbance spectrum of the drug postinjection was recorded over time (up to 2 days p.i.). The in vivo drug absorption spectrum was best displayed by determining the ratio of the postinjection spectrum to the preinjection spectrum in the tumor versus the skin. This experiment also determined the wavelength and time at which to perform in vivo PDT treatments.

Determination of In Vivo Photosensitizing Activity. The day before PDT light treatment, the mice with a tumor $\sim 4\text{--}5\text{ mm}^3$ in diameter were injected intravenously with 0.2–1.0 $\mu\text{mol/kg}$ of the photosensitizer (photosensitizers were diluted in 1% Tween 80 in HBSS; Sigma), and the hair over the treatment spot was removed via depilation (with Nair). At 24 h p.i., the mice (10 per group) were restrained in plastic plexiglass holders without anesthesia, treated with a 1 cm^2 drug-activating laser light spot from an argon-pumped dye laser for a total fluence of 135 J/cm^2 at a fluence rate of 75 mW/cm^2 (total power of 59–60 mW for a 30 min treatment). The DCM Ext dye (Exciton, Dayton, OH) and the Styryl 8 dye (Exciton, Dayton, OH – LDS 751) yielded tunable wavelengths from 682 to 745 nm and 720–835 nm, respectively. The laser beam was passed through an eight-way beam splitter. The power (in mW) at each individual fiber could be individually set using the Brewster-window-type attenuators and was constantly monitored during the treatment. Post-PDT, the mice were observed daily, the tumors were measured using two orthogonal measurements, L and W (perpendicular to L), and the volumes were calculated, using the formula $V = L \cdot W^2/2$, and recorded. Mice were considered cured if there was no palpable tumor by day 60.

Statistical Evaluation. All in vitro data were presented as the mean of three replicate experiments with the standard deviation of each. The GraphPad Prism program (v.3.0) was used for all in vivo tumor response (Kaplan–Meier plots).²³

Acknowledgment. Authors are thankful to Dr. Guolin Li for his initial help in preparing the purpurinimide–aminobenzyl–DTPA conjugate and to Dr. Janet Morgan and Dr. David Bellnier for valuable discussions. The financial support from the NIH (CA55791) and the shared resources of the RPCI support grant (P30CA16056) is highly appreciated. A.L.G. thanks the National Science Foundation under the Integrative Graduate Education and Research Traineeship (Grant DGE0114330) for funding the graduate fellowship. We thank the Mass Spectrometry Facility, Roswell Park Cancer Institute, Buffalo, and the Michigan State University for analyzing our samples.

Supporting Information Available: ^1H NMR spectra of compounds 4–10, 13–20, 19S, and 26 and HPLC chromatograms of compounds 6–11, 13, 14, 18–21, 24, and 26. This material is available free of charge from <http://pubs.acs.org>.

References

- Moore J. V.; West C. M.; Whitehurst, C. The biology of photodynamic therapy. *Phys. Med. Biol.* **1997**, *42*, 913–935.
- Morton C. A. Topical photodynamic therapy in dermatology. *S. Afr. Med. J.* **2001**, *91*, 636–637.
- Ochsner, M. Photodynamic therapy: The clinical perspective. Review on applications for control of diverse tumorous and non-tumorous diseases. *Arzneim.-Forsch.* **1997**, *47*, 1185–1194.
- Sherman, W. M.; Allen, C. M.; van Lier, J. E. Role of activated species in photodynamic therapy. *Methods Enzymol.* **2000**, *319*, 376–400.
- (a) Pandey, R. K.; Shiau, F. Y.; Dougherty, T. J.; Smith, K. M. Regioselective synthesis of ether linked porphyrin dimers and trimers related to Photofrin II. *Tetrahedron* **1991**, *47*, 9571–9584. (b) Kessel, D.; Thompson, R.; Musselman, B.; Chang, C. K. *Cancer Res.* **1987**, *47*, 4642–4745. (c) Pandey, R. K.; Dougherty, T. J. Synthesis and photosensitizing activity of porphyrins joined with ester linkages. *Cancer Res.* **1989**, *49*, 2042–2047. (d) Pandey, R. K.; Shiau, F. Y.; Medforth, C. J.; Dougherty, T. J.; Smith, K. M. An efficient synthesis of porphyrin dimers linked with carbon-carbon linkages. *Tetrahedron Lett.* **1990**, *31*, 789–792.
- Pandey, R. K. Recent advances in photodynamic therapy. *J. Porphyrins Phthalocyanines* **2000**, *4*, 368–373.
- Wohrle, D.; Hirth, A.; Bogdahn-Rai, T.; Schnurpfeil, G.; Shopova, M. Photodynamic therapy of cancer: Second and third generations of photosensitizers. *Russ. Chem. Bull.* **1998**, *47*, 807–816.
- Pandey, R. K.; Zheng, G. In *The Porphyrin Handbook*; Kadish, K. M., Smith, K. M., Guillard, R., Eds.; Academic Press: Boston, 2000; Vol. 8, Chapter 43.
- Chen, Y.; Graham, A.; Potter, W.; Morgan, J.; Vaughan, L.; Bellnier, D. A.; Henderson, B. W.; Oseroff, A.; Dougherty, T. J.; Pandey, R. K. Bacteriopurpurinimides: Highly stable and potent photosensitizers for photodynamic therapy. *J. Med. Chem.* **2002**, *45*, 255–258.
- Wilson, B. C.; Farrell, T. J.; Patterson, M. S. An optical fiber-based diffuse reflectance spectrometer for non-invasive investigations of photodynamic sensitizers *in vivo* (In future directions and applications in photodynamic therapy). *Proc. SPIE Int. Soc. Opt. Eng.* **1990**, *156*, 219–481.
- Pandey, R. K.; Sumlin, A. B.; Potter, W. R.; Bellnier, D. A.; Henderson, B. W.; Constantine, S.; Aoudia, M.; Rodgers, M. A. J.; Smith, K. M.; Dougherty, T. J. Synthesis, photophysical properties and photodynamic efficacy of alkyl ether analogs of chlorophyll-a derivatives. *Photochem. Photobiol.* **1996**, *52*, 194–205.
- Henderson, B. W.; Bellnier, D. A.; Greco, W. R.; Sharma, A.; Pandey, R. K.; Vaughan, L.; Weishaupt, K. R.; Dougherty, T. J. A Quantitative structure-activity relationship for a congeneric series of pyropheophorbide derivatives as photosensitizers for photodynamic therapy. *Cancer Res.* **1997**, *47*, 4000–4007.
- Zheng, G.; Potter, W. R.; Camacho, S. H.; Missert, J. R.; Wang, G.; Bellnier, D. A.; Henderson, B. W.; Rodgers, M. A. J.; Dougherty, T. J.; Pandey, R. K. Synthesis, photophysical properties, tumor uptake and preliminary in vivo photosensitizing efficacy of a homologous series of 3-(1'-alkyloxy)ethyl-3'-vinylpurpurin-18-N-alkylimides with variable lipophilicity. *J. Med. Chem.* **2001**, *44*, 1540–1559.
- Zheng, G.; Potter, W. R.; Sumlin, A.; Dougherty, T. J.; Pandey, R. K. Photosensitizers related to purpurin-18-N-alkylimides: A comparative in vivo tumoricidal ability of ester versus amide functionalities. *Bioorg. Med. Chem. Lett.* **2000**, *10*, 123–127.
- Prakash, G. K. S.; Yudin, A. K. Perfluoroalkylation with organosulfon reagents. *Chem. Rev.* **1997**, *97*, 757–786.
- Banks, R. E.; Smart, B. E.; Tatlow, J. C. *Organofluorine Chemistry—Principles and Commercial Applications*; Plenum Press: New York, 1994.
- Thayer, A. M. Constructing life sciences compounds. *Chem. Eng. News* **2006**, *84* (23), 27.
- Gryshuk, A. L.; Graham, A.; Pandey, R. K.; Potter, W. R.; Missert, J. R.; Oseroff, A.; Dougherty, T. J.; Pandey, R. K. A first comparative study of purpurinimide-based fluorinated versus nonfluorinated photosensitizers for photodynamic therapy. *Photochem. Photobiol.* **2002**, *76* (5), 83–87.
- Demas, J. N.; Harris, E. W.; McBride, R. P. Energy transfer from luminescent transition metal complexes to oxygen. *J. Am. Chem. Soc.* **1977**, *99*, 3547–3551.
- Morgan, J.; Potter, W. R.; Oseroff, A. R. Comparison of photodynamic targets in a carcinoma cell line and its mitochondrial DNA-deficient derivative. *Photochem. Photobiol.* **2000**, *70*, 747–757.
- Patterson, M. S.; Schwartz, E.; Wilson, B. C. Quantitative reflectance spectroscopy for the non-invasive measurement of photosensitizer concentration in tissue during photodynamic therapy. *Proc. SPIE Int. Soc. Opt. Eng.* **1989**, *1065*, 114–122.
- Peng, Q.; Moan, J.; Nesland, J. M. Correlation of subcellular and intratumoral photosensitizer localization with ultrastructural features after photodynamic therapy. *Ultrastruct. Pathol.* **1996**, *20*, 109–129.
- Kaplan, E. L.; Meier, P. Nonparametric estimation from incomplete observations. *J. Am. Stat. Assoc.* **1958**, *53*, 457–481.
- Chen, Y.; Sumlin, A.; Morgan, J.; Gryshuk, A.; Oseroff, A.; Henderson, B. W.; Dougherty, T. J. and Pandey, R. K. Synthesis and photosensitizing efficacy of isomerically pure bacteriopurpurinimides. *J. Med. Chem.* **2004**, *47*, 4814–4817 and references therein.
- Corey, E. J.; Bakshi, R. K.; Shibata, S.; Chen, C. P.; Singh, V. A. A stable and easily prepared catalyst for the enantioselective reduction of ketones. Applications to multiple synthesis. *J. Am. Chem. Soc.* **1987**, *109*, 7925–7926.